NASA/TM-1999-209114

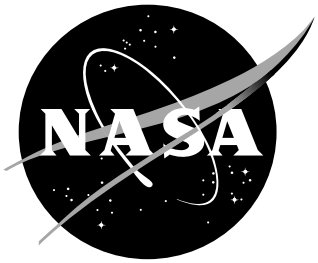

Two-Dimensional Fourier Transform Applied to Helicopter Flyover Noise

Odilyn L. Santa Maria
Langley Research Center, Hampton, Virginia

March 1999

The NASA STI Program Office ... in Profile

Since its founding, NASA has been dedicated to the advancement of aeronautics and space science. The NASA Scientific and Technical Information (STI) Program Office plays a key part in helping NASA maintain this important role.

The NASA STI Program Office is operated by Langley Research Center, the lead center for NASA's scientific and technical information. The NASA STI Program Office provides access to the NASA STI Database, the largest collection of aeronautical and space science STI in the world. The Program Office is also NASA's institutional mechanism for disseminating the results of its research and development activities. These results are published by NASA in the NASA STI Report Series, which includes the following report types:

- TECHNICAL PUBLICATION. Reports of completed research or a major significant phase of research that present the results of NASA programs and include extensive data or theoretical analysis. Includes compilations of significant scientific and technical data and information deemed to be of continuing reference value. NASA counterpart of peer-reviewed formal professional papers, but having less stringent limitations on manuscript length and extent of graphic presentations.

- TECHNICAL MEMORANDUM. Scientific and technical findings that are preliminary or of specialized interest, e.g., quick release reports, working papers, and bibliographies that contain minimal annotation. Does not contain extensive analysis.

- CONTRACTOR REPORT. Scientific and technical findings by NASA-sponsored contractors and grantees.

- CONFERENCE PUBLICATION. Collected papers from scientific and technical conferences, symposia, seminars, or other meetings sponsored or co-sponsored by NASA.

- SPECIAL PUBLICATION. Scientific, technical, or historical information from NASA programs, projects, and missions, often concerned with subjects having substantial public interest.

- TECHNICAL TRANSLATION. English-language translations of foreign scientific and technical material pertinent to NASA's mission.

Specialized services that complement the STI Program Office's diverse offerings include creating custom thesauri, building customized databases, organizing and publishing research results ... even providing videos.

For more information about the NASA STI Program Office, see the following:

- Access the NASA STI Program Home Page at *http://www.sti.nasa.gov*

- E-mail your question via the Internet to help@sti.nasa.gov

- Fax your question to the NASA STI Help Desk at (301) 621-0134

- Phone the NASA STI Help Desk at (301) 621-0390

- Write to:
  NASA STI Help Desk
  NASA Center for AeroSpace Information
  7121 Standard Drive
  Hanover, MD 21076-1320

NASA / TM-1999-209114

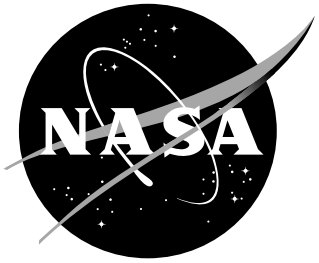

Two-Dimensional Fourier Transform Applied to Helicopter Flyover Noise

Odilyn L. Santa Maria
Langley Research Center, Hampton, Virginia

National Aeronautics and
Space Administration

Langley Research Center
Hampton, Virginia 23681-2199

March 1999

Available from:

NASA Center for AeroSpace Information (CASI)
7121 Standard Drive
Hanover, MD 21076-1320
(301) 621-0390

National Technical Information Service (NTIS)
5285 Port Royal Road
Springfield, VA 22161-2171
(703) 605-6000

ABSTRACT

A method to separate main rotor and tail rotor noise from a helicopter in flight is explored. Being the sum of two periodic signals of incommensurate frequencies, helicopter noise is neither periodic nor stationary, but possibly harmonizable. The traditional single Fourier transform puts the signal energy into frequency bins whose size depends on the lengths of the data blocks chosen. Incommensurate frequencies would not be adequately represented because any data block chosen would favor one frequency or the other. A two-dimensional Fourier analysis method is used to show helicopter noise as harmonizable.

The two-dimensional spectral analysis method is first applied to simulated signals: a single tone, a series of periodically correlated tones, and a series of tones composed of two tones of incommensurate frequencies and their harmonics. This initial analysis gives an idea of the characteristics of the two-dimensional autocorrelations and spectra.

Data from a helicopter flight test is analyzed in two dimensions. The test aircraft are a Boeing MD902 Explorer (no tail rotor) and a Sikorsky S-76C+ (4-bladed tail rotor). Data blocks of length equivalent to integer multiples of the main rotor blade passage are used in the analysis. The results show that the main rotor and tail rotor signals can indeed be separated in the two-dimensional Fourier transform spectrum. The separation occurs along the diagonals associated with the frequencies of interest. These diagonals are individual spectra containing only information related to one particular frequency.

TABLE OF CONTENTS

LIST OF FIGURES

LIST OF SYMBOLS

a_j	Constant coefficient for correlation autoregressive process
A	Amplitude component of autocorrelation, $R_x(t)$
B	Amplitude component of autocorrelation, $R_x(t)$
$E[\bullet]$	Expected value
$\hat{E}$	Fourier transform of expected value
g	Variable of characteristic equation
p	Period
R_x	Autocorrelation of random process X
S_x	Fourier transform of random process X
t	Time
T	Period
$X(t)$	Random process
Y	Periodic signal
Z	Periodic signal
α	Frequency variable
β	Frequency variable
δ	Dirac delta function
λ	Frequency variable in two-dimensional Fourier transform
ω	Frequency in radians

Subscripts:

m	Integer variable
n	Integer variable

ACKNOWLEDGEMENTS

Technical tasks described in this document include tasks supported with shared funding by the U.S. rotorcraft industry and government under the RITA/NASA Cooperative Agreement No. NCCW-0076, Advanced Rotorcraft Technology, Aug. 15, 1995.

The author wishes to express sincere gratitude for support and guidance to the faculty and staff of the Graduate Program in Acoustics at Penn State, especially Dr. Philip Morris, and the members of the Fluid Mechanics and Acoustics Division at NASA Langley Research Center, especially Dr. Jay C. Hardin (ret.) and Dr. Feri Farassat.

CHAPTER I

INTRODUCTION

The sound of a helicopter flying overhead is one that most people can identify. Its distinctive noise is a cause of annoyance to the listener on the ground, and therefore could be considered a high impact community noise source. The first step in the process of reducing far field helicopter noise is its characterization. This involves identifying:

- where on the aircraft the noise is being generated;
- what condition the aircraft is flying when the noise is generated;
- how the noise propagates to the ground.

This information can be used to create an illustration or graphic that visualizes the acoustics of a helicopter. The graphic would then be a tool used to identify the areas (flight operations, blade tips, etc) to modify in order to reduce the noise for the listener. The researcher is thus challenged to create this illustration or graphic that efficiently conveys the most relevant information.

The purpose of this paper is to identify the advantages of using a two-dimensional Fourier transform in the analysis of helicopter flyover noise.

Sources of helicopter noise

Figure 1, from a NASA Langley chart, illustrates the sources of helicopter noise for a helicopter with a tail rotor. These sources of helicopter noise and their physical meaning are defined in [1] and are briefly described below.

Periodic Noise

Periodic or harmonic noise from a helicopter comes in various forms: thickness noise, noise from blade-vortex interaction, tail rotor noise, and the noise from main rotor-tail rotor interaction. Periodic noise mechanisms are a function of the rotational speed of rotating devices such as the rotor. Thickness noise is caused by the movement of air displaced by the rotating blade, and propagates predominantly in the rotor plane. The

extreme case of thickness noise, when the tip speeds of the advancing blades are close to transonic, is call high speed impulsive noise (HSI). HSI generally occurs in level flight.

Blade-vortex interaction (BVI) noise, also called blade slap, is generated when the tip-trailing vortex shed at a rotor blade tip impacts the other rotor blades. Trailing vortices usually travel downward and are intersected in descending flight.

Loading noise is caused by the lift and drag forces acting on the rotating blade and can be periodic in nature. Compressor noise from the helicopter engine is also periodic, with a much higher frequency than the main rotor noise. Tail rotor noise and main rotor-tail rotor interaction noise are described further below.

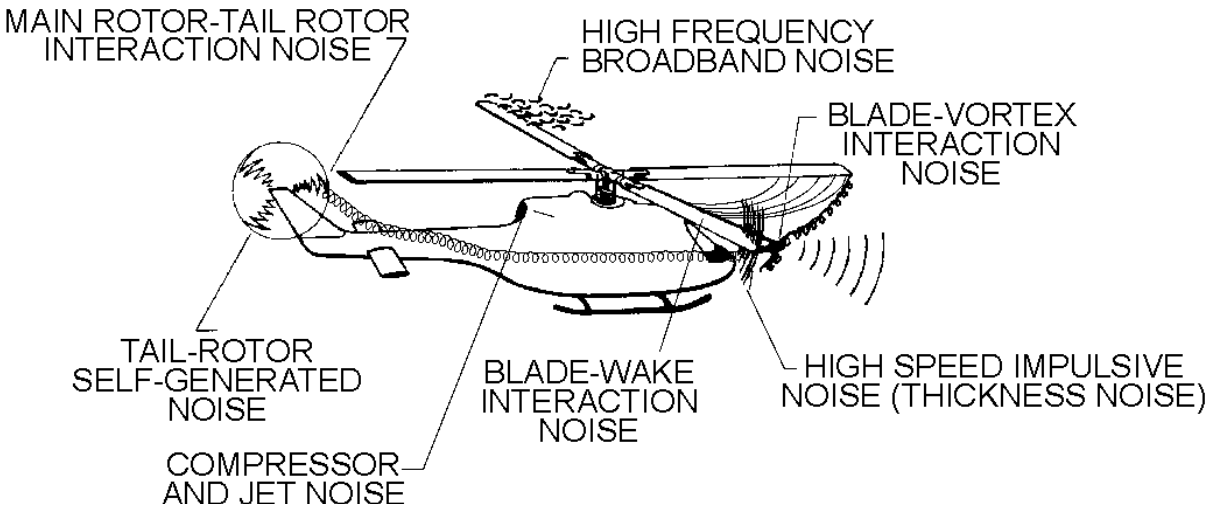

Figure 1. Helicopter noise sources

Broadband Noise

Some broadband noise is caused by turbulence interacting with the rotor blades. The resulting noise is broadband in nature because the generating mechanism, turbulence, randomly impacts the rotor blades. Turbulence in the boundary layer of the rotor blade causes self-noise, as does the flow over the sharp trailing edge of the rotor blade. Turbulence ingested from the atmosphere also produces broadband noise when the rotor blades cut through it. Blade-wake interaction is another cause of broadband noise, as the

turbulent wake from a preceding blade impacts the following blades. Jet noise emanates from the helicopter engines and is heard mostly aft of the aircraft.

This thesis addresses the periodic noise of helicopters, focusing on those frequencies associated with the main rotor and tail rotor rotation.

To explore the possibilities of the two-dimensional Fourier transform, this thesis will provide the two-dimensional spectra from two different helicopters: one with a tail rotor, and one without. These data, collected during an acoustic flight test in 1996, will be shown using conventional analysis methods, namely the FFT, as well as with the two-dimensional Fourier transform. The two-dimensional Fourier transform will be used as an alternate method to distinguish main rotor and tail rotor noise.

Noise of the Main Rotor

As shown in Fig. 1, the main rotor generates noise in several ways: 1) high frequency broadband noise, 2) thickness noise, 3) blade-vortex interaction noise, 4) blade-wake interaction noise, 5) loading noise.

Many studies have been conducted to identify, predict, and measure these different sources of main rotor noise. Some studies have targeted the wakes and tip vortices shed by the main rotor blades. These wakes and tip vortices not only generate blade-wake interaction and the highly impulsive blade-vortex interaction noise when they encounter other main rotor blades, but they can also encounter the tail rotor blades and generate main rotor-tail rotor interaction noise. This latter phenomenon will be discussed in more detail below.

Noise of the Tail Rotor

The tail rotor itself is a smaller main rotor and thus generates the same types of noise as the main rotor. However, due to its orientation on the aircraft, its surrounding flow field in forward flight is quite different from that of the main rotor. It is not only ingesting atmospheric turbulence, it is also encountering wakes and vortices from the main rotor, hub, and fuselage. Also, due to its orientation, any noise generated in the tail

rotor tip path plane would propagate to the ground directly underneath the tail. References [4], [5], [6], and [7] address tail rotor noise. This type of noise was observed to be strongest during takeoff for the Sikorsky S-76 in Ref. [7].

Main Rotor-Tail Rotor Interaction Noise

Noise generated by main rotor-tail rotor interaction has been shown to be significant [8]. Figure 1 illustrates the tip vortex shed from a main rotor blade intersecting the tail rotor tip path plane. Not shown is the wake from from the main rotor blade, which also may intersect the tail rotor tip path plane.

The generation of main rotor-tail rotor interaction noise is dependent on the helicopter flight track. Reference [8] referred to this noise as a "burbling" sound, highly annoying to the listener, and also very dependent on the type of aircraft maneuver. In both references [7] and [8], main rotor-tail rotor interaction noise was identified on power density spectra as sums or differences of multiples of the main rotor and tail rotor harmonics. Although evidence of main rotor-tail rotor interaction noise appears in the data analyzed in Chapter 6, it will not be addressed in detail in this thesis.

Periodicity of Helicopter Noise

The main rotor-tail rotor ratio, the multiple of tail rotor rotational frequency in relation to the main rotor rotational frequency, is never designed to be a whole number. This prevents the harmonics of the two rotors from reinforcing each other and resonating. Thus the noise from these two rotors can be characterized as the sum of two periodic sinusoids with incommensurate frequencies. It is shown in [3] that this summed signal is theoretically not periodic and cannot be adequately represented by the single Fourier transform. Therefore, Hardin and Miamee proposed in [3] that a two-dimensional Fourier transform would better characterize the signal.

The following chapter discusses the two-dimensional Fourier transform and explains how it may be used to distinguish main rotor noise from tail rotor noise more clearly. Chapter 3 shows preliminary two-dimensional Fourier transform analyses performed on simulated signals to indicate what "ideal" two-dimensional spectra should

look like. Chapter 4 describes the helicopter acoustics flight test from which data is analyzed. Chapter 5 shows the results of two-dimensional Fourier transform analysis on the measured flyover data, followed by conclusions in Chapter 6. The advantages of two-dimensional Fourier transform analysis on helicopter flyover acoustic data are discussed in Chapter 6, and suggestions for future study are also presented.

CHAPTER 2

TWO-DIMENSIONAL FOURIER TRANSFORM

Random Processes

Hardin and Miamee [3] define a class of random processes called correlation autoregressive, or CAR. The CAR process, $X(t)$, with autocorrelation function $R_x(t_1,t_2) = E[X(t_1)X(t_2)]$, is given by the relationship

$$R_x(t_1,t_2) = \sum_{j=1}^{N} a_j R_x(t_1+\tau_j, t_2+\tau_j) \qquad (1)$$

for all t_1 and t_2, where a_j and τ_j are fixed real numbers and N is a fixed, positive integer. Subsets of CAR processes – stationary, periodically correlated, harmonizable – are defined in [3] by the behavior of the autocorrelation in eq. 1. Figure 2 shows a Venn diagram from [3], representing these classes of random processes.

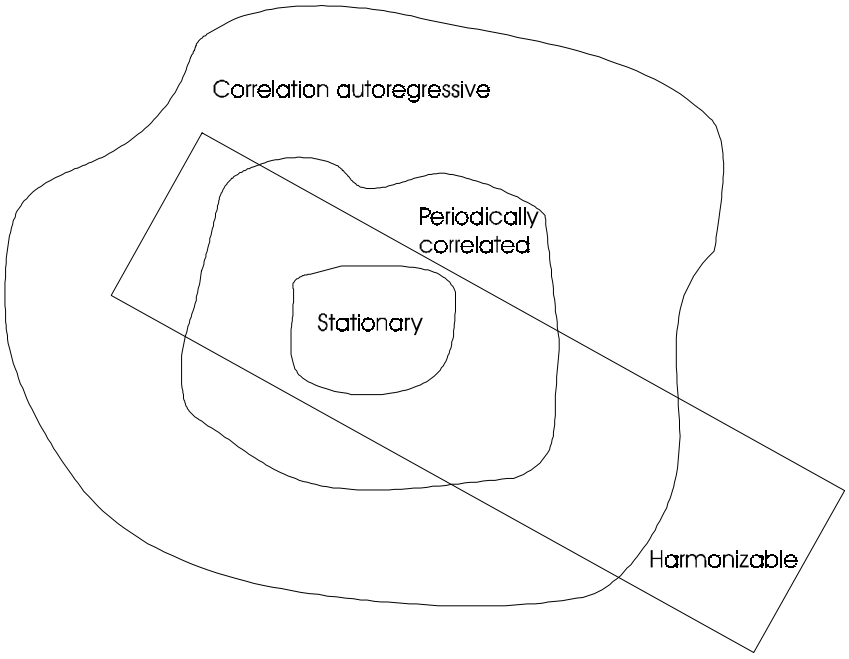

Figure 2. Venn diagram of class relations [3].

A stationary random process is defined in [3] as a random process where

$$R_x(t_1,t_2)=\sum_{j=1}^{N} a_j R_x(t_1+t,t_2+t)=R_x(t_1,t_2)\sum_{j=1}^{N} a_j \quad \text{for all t.} \tag{2}$$

A periodically correlated process is one such that

$$R_x(t_1,t_2)=R_x(t_1+np,t_2+np)=R_x(t_1,t_2)\sum_{j=1}^{N} a_j \quad \text{for all n.} \tag{3}$$

This type of process essentially repeats itself over a finite period *p*. For both stationary and periodically correlated random processes to satisfy eq. 1, $\sum_{j=1}^{N} a_j = 1$.

An example of a stationary, periodically correlated process, is that of a sinusoid. Consider a sinusoidal signal, *X(t)*, of finite length with frequency 20 Hz. This signal is shown in Fig. 3(a). Figure 3(b) shows the autocorrelation of the signal, and part (c) shows its autospectrum. The period of this signal is $T=\frac{1}{f}=0.05\text{sec}$ as can be readily seen in Fig. 3 (a). A Hanning window was used in calculating the autocorrelation (b) and autospectrum (c). The Hanning window tapers down the amplitude at the beginning and the end of a signal in order to better match these termination points. It is used extensively in analysis of periodic signals.

The autocorrelation shown in Fig. 3(b) is plotted as a function of the time $t=t_2-t_1$. It appears as a damped sinusoid due to the finite length of the signal and windowing effects. An infinitely long and continuous sinusoid would produce a sinusoid for the autocorrelation and a delta function for the Fourier transform. Since the signal in Fig. 3(a) is discrete and finite, the autocorrelation is damped and the Fourier transform shows a gradual peak near 20 Hz.

Helicopter noise was classified in [3] as a harmonizable, correlation autoregressive random process. For a helicopter with a tail rotor, there are two periodic signals with incommensurate frequencies. This type of signal can be considered neither stationary nor periodic. For example, consider a signal *X(t)*, that is the sum of two sinusoids, *Y(t)* + *Z(t)*.

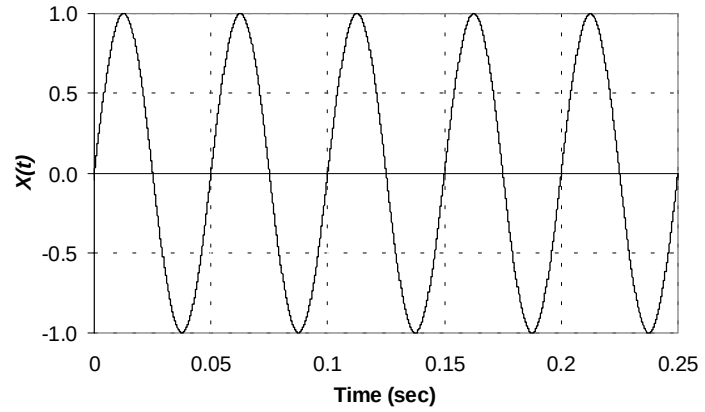

(a) Sinusoidal signal, *X(t)*

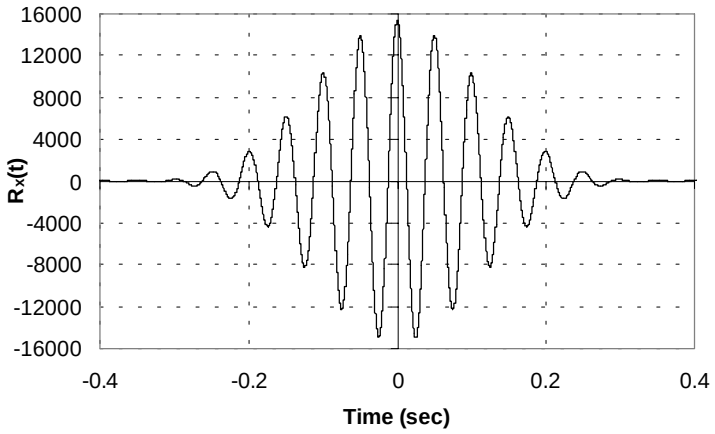

(b) Autocorrelation, R_x, of *X(t)*.

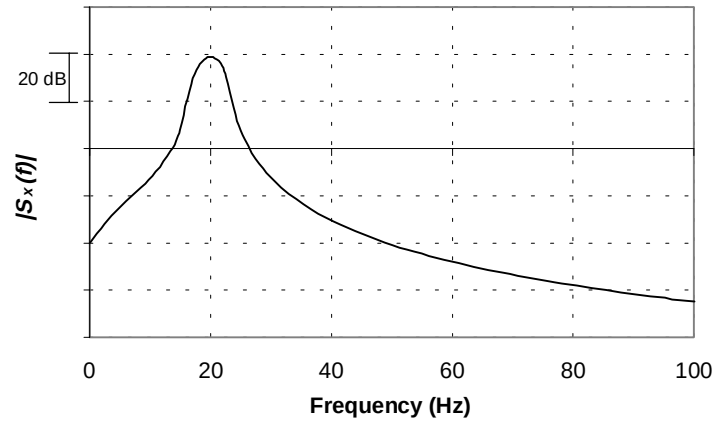

(c) Amplitude of Autospectrum, $S_x(f)$ of *X(t)*.

Figure 3. Stationary and periodically correlated process.

Figure 4 (a) shows the signal, *X(t)*. Figure 4(b) shows the autocorrelation of the signal, and Fig. 4(c) shows its autospectrum. A Hanning window has been used in the calculation of the autocorrelation and autospectrum of *X(t)*. Although this signal appears to repeat itself, the signal is not periodic. In fact, since the Fourier transform and autocorrelation of a correlation autoregressive process such as *X(t)* is a function of two variables, t_1 and t_2 [3], one-dimensional plots as shown in Fig. 4 (a) and (b) are not completely representative of the process. Rather, these plots have been produced assuming the signal is stationary.

To show that the signal *X(t)* in Fig. 4(a) is not periodic, examine the sum of two sinusoids that are periodic with period *p*. Given two frequencies α and β, then for a periodic signal,

$$\sin \alpha t + \sin \beta t = \sin \alpha (t + p) + \sin \beta (t + p)$$
$$\sin \alpha t + \sin \beta t = \sin \alpha t \cos \alpha p + \cos \alpha t \sin \alpha p + \sin \beta t \cos \beta p + \cos \beta t \sin \beta p$$

This is true if and only if

$$\cos \alpha p = \cos \beta p = 1 \quad \text{and} \quad \sin \alpha p = \sin \beta p = 0 .$$

Thus, the signal is periodic if and only if

$$\alpha p = 2m\pi \quad \text{and} \quad \beta p = 2n\pi .$$

This type of signal, the sum of two periodic signals with incommensurate frequencies, would not be ideally represented by the single Fourier transform, which breaks a signal in the time domain into a series of sinusoids represented in the frequency domain. The finite Fourier transform treats the signal as if it were periodic with period equal to the block length. A periodic signal is thus best represented when the block length is chosen as an integer multiple of the period. When the two sinusoids are of incommensurate frequencies, any period chosen as the block length will result in an error. The errors for a non-periodic process are derived in Ref. [9]. Additionally, because the simulated signal in Fig. 4 is the sum of two "pure tones," it lacks any interaction between these tones, i.e., main rotor-tail rotor interaction.

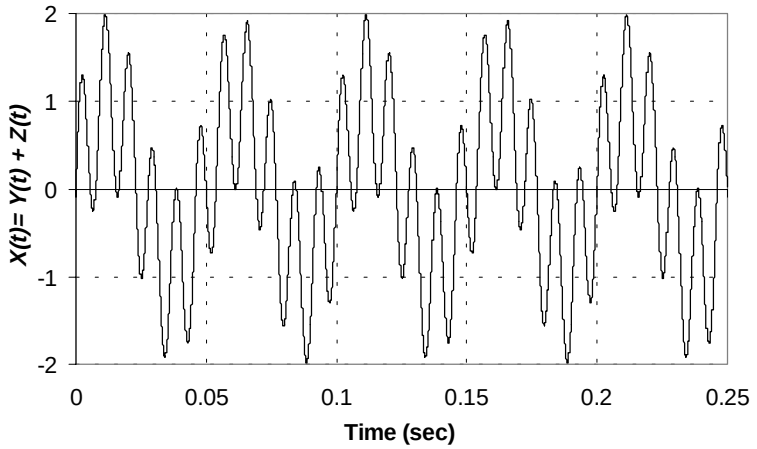

(a) Time history, *X(t)*

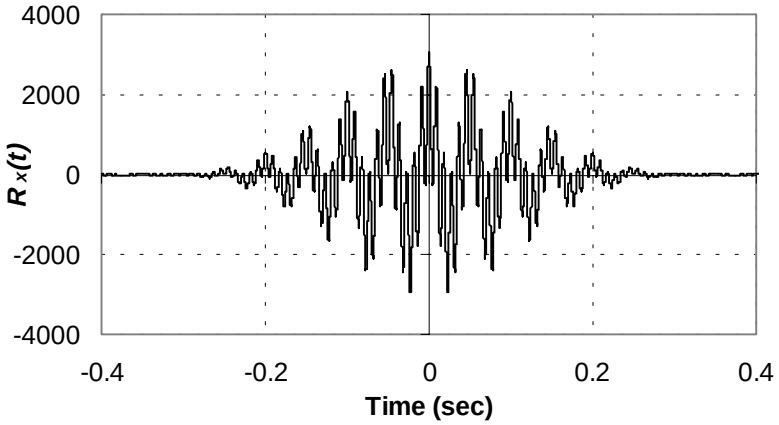

(b) Autocorrelation, $R_x(t)$, of *X(t)*.

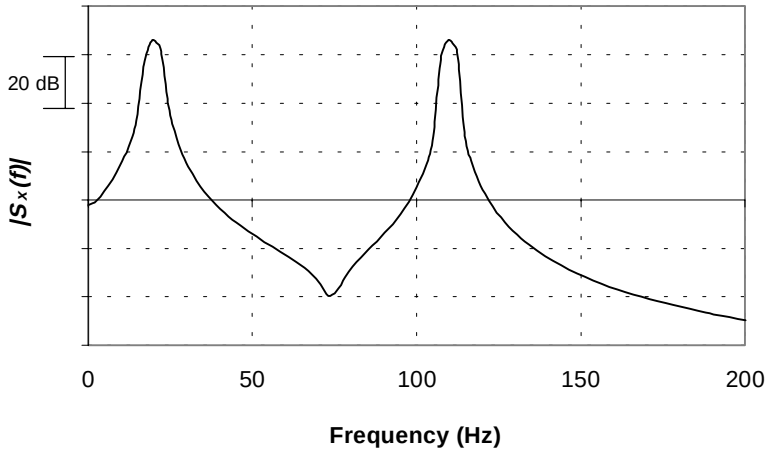

(c) Amplitude of Autospectrum, $S_x(f)$, of *X(t)*.

Figure 4. Sum of two sinusoids with frequencies of 22 and 121 Hz

The next section explains that despite being neither stationary nor periodically correlated, the signal from Fig. 4 and helicopter noise may be considered harmonizable, and thus be analyzed using techniques based on periodicity.

Harmonizability

Reference [3] defines a harmonizable process as one in which the two-dimensional Fourier transform, $S_x(\omega_1,\omega_2)$ of its autocorrelation, $R_x(t_1,t_2)$, exists. The two-dimensional Fourier transform, also called the two-dimensional power spectral density of a random process, is defined in [10] as

$$S_x(\lambda_1,\lambda_2)=\int_{-\infty}^{\infty}\int_{-\infty}^{\infty}R_x(t_1,t_2)e^{-j(\lambda_1 t_1-\lambda_2 t_2)}dt_1dt_2 \tag{4}$$

Given a process of two time variables, *X(t)*, its two-dimensional autocorrelation, $R_x(t_1,t_2)$ would be

$$R_x(t_1,t_2)=E[X(t_1)X(t_2)] \tag{5}$$

where $E[\cdot]$ is the expected value.

To understand the content of a two-dimensional Fourier transform for the case of the sum of two periodic signals with incommensurate frequencies, let

$$X(t)=A_1e^{i\omega_1 t}+A_2e^{i\omega_2 t} \tag{6}$$

If the two-dimensional autocorrelation is obtained, the result is a sum of four terms involving the two time variables, and the two frequency variables,

$$E[X(t_1)X(t_2)]=A_1^2e^{i\omega_1(t_1+t_2)}+A_2^2e^{i\omega_2(t_1+t_2)}+A_1A_2e^{i(\omega_1t_1+\omega_2t_2)}+A_1A_2e^{i(\omega_2t_1+\omega_1t_2)} \tag{7}$$

The two-dimensional Fourier transform, $\hat{E}$, of eq. 7 can be expressed as

$$\hat{E}=A_1^2\hat{e}^{i\omega_1(t_1+t_2)}+A_2^2\hat{e}^{i\omega_2(t_1+t_2)}+A_1A_2\hat{e}^{i(\omega_1t_1+\omega_2t_2)}+A_1A_2\hat{e}^{i(\omega_2t_1+\omega_1t_2)} \tag{8}$$

where

$$\hat{e}^{i\omega_1(t_1+t_2)} = \int_{-\infty}^{\infty}\int_{-\infty}^{\infty} e^{i\omega_1(t_1+t_2)}\, e^{-i(\lambda_1 t_1+\lambda_2 t_2)} dt_1 dt_2 = \delta(\omega_1-\lambda_1)\delta(\omega_1-\lambda_2), \tag{9}$$

$$\hat{e}^{i\omega_2(t_1+t_2)} = \delta(\omega_2-\lambda_1)\delta(\omega_2-\lambda_2),$$

$$\hat{e}^{i(\omega_1 t_1+\omega_2 t_2)} = \delta(\omega_1-\lambda_1)\delta(\omega_2-\lambda_2),$$

$$\hat{e}^{i(\omega_2 t_1+\omega_1 t_2)} = \delta(\omega_2-\lambda_1)\delta(\omega_1-\lambda_2).$$

δ is the Dirac delta function, λ_1 and λ_2 are the frequency variables, and ω_1 and ω_2 are incommensurate frequencies.

Hardin and Miamee proved theoretically in [3] that the two-dimensional spectrum of a harmonizable, correlation autoregressive process would feature "support only on lines $\omega_1-\omega_2=r_k$ parallel to the line $\omega_1=\omega_2$, with the r_k's being the real roots of the characteristic equation

$$g(\Omega)=\sum_{j=1}^{N} a_j e^{-i\Omega\tau_j} - 1 = 0. \tag{10}$$

where $\Omega=\omega_1-\omega_2$.

These "supports" are shown in fig. 5, reproduced from [3]. As shown in fig. 5, the two-dimensional power spectral density for a harmonizable, correlation autoregressive process is zero everywhere except on the diagonal, $\omega_1=\omega_2$, and parallel lines as described above. From eq. 8, it can be determined that these parallel lines can only be dependent on ω_1 and ω_2. However, if ω_1 and ω_2 are incommensurate, the only parallel lines that would appear would be those relating to the first two terms of eq. 8. That is, the parallel lines would be exclusively representative of ω_1 or ω_2. Note that this condition would apply to all harmonizable processes, not just those with two incommensurate frequencies.

For a finite signal, the Fourier transform of eq. 7 is [from eq. 9]

$$\hat{E}(\lambda_1,\lambda_2)=\sum_{m=1}^{N}\sum_{n=1}^{N}\begin{bmatrix} A_m A_n \delta(\lambda_1-n\omega_1)\delta(\lambda_2-m\omega_1)+A_n B_m \delta(\lambda_1-n\omega_1)\delta(\lambda_2-m\omega_2) \\ +A_m B_n \delta(\lambda_1-n\omega_2)\delta(\lambda_2-m\omega_1)+B_m B_n \delta(\lambda_1-n\omega_2)\delta(\lambda_2-m\omega_2)\end{bmatrix} \tag{11}$$

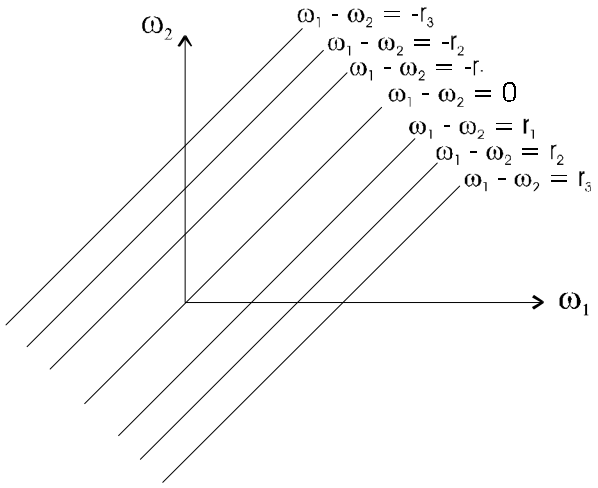

Figure 5. Support of 2-D power spectral density [3].

Thus, the amplitudes of the diagonals illustrated in Fig. 5 would be products of different combinations of A_m, A_n, B_m, and B_n. These amplitudes along the main or center diagonal would be for the case m=n. It would then be possible from these center diagonal amplitudes to break down the different components of the amplitude of the parallel diagonals. This field of amplitude components will not be applied to the data in this paper. It is simply introduced as a subject for further study.

The next chapter gives some examples of two-dimensional Fourier transform spectra from simulated signals. These provide some idea of the characteristics of two-dimensional spectra of very simple signals, thus giving a simplistic preview of expected spectra of real helicopter signals.

CHAPTER 3

RESULTS WITH SIMULATED SIGNALS

To get an idea of the expected results from the experimental data, it is useful to work initially with simulated or computer-generated data. In the following sections, two-dimensional spectra will be presented from a pure tone, a periodically correlated signal, and a non-periodic signal. Since two-dimensional spectral values are generally complex, the amplitude of the spectra will be shown.

All two-dimensional calculations are made using a sampling rate of 5000 Hz and a rectangular window, as opposed to 20000 Hz sampling rate and Hanning windows for the one-dimensional calculations. The sample length of the two-dimensional autocorrelations and spectra are multiples of the fundamental frequency of 20 Hz, while the one-dimensional spectra use 8192 points. The lower sampling rate allows higher multiples of the fundamental frequency to be used while retaining computing speed and frequency resolution. Multiples of the fundamental frequency at 20 Hz are used for better resolution in the two-dimensional values.

Pure tone

The pure tone generated using MATLAB software in fig. 3 has been used to generate the two-dimensional spectrum. Using MATLAB, the power spectral estimation (Eq. 5) described in Chapter 2 is used to generate the two-dimensional power density spectrum shown in Fig. 6. From Eq. 5, it is apparent that the diagonal of the spectrum in Fig. 6 is equivalent to the single Fourier transform spectrum that is shown in Fig. 3(c).

Periodically Correlated Signal

A periodically correlated signal consisting of a pure tone and harmonics with decreasing amplitude has also been generated, using MATLAB. For this example, 19

harmonics in addition to the fundamental at 20 Hz are generated, using the following equation:

$$X(t) = \sum_{i}^{20} (1 - .01i) \sin(2\pi 20it) \tag{12}$$

where t = 0 to 409.4 msec in increments of 0.2 msec.

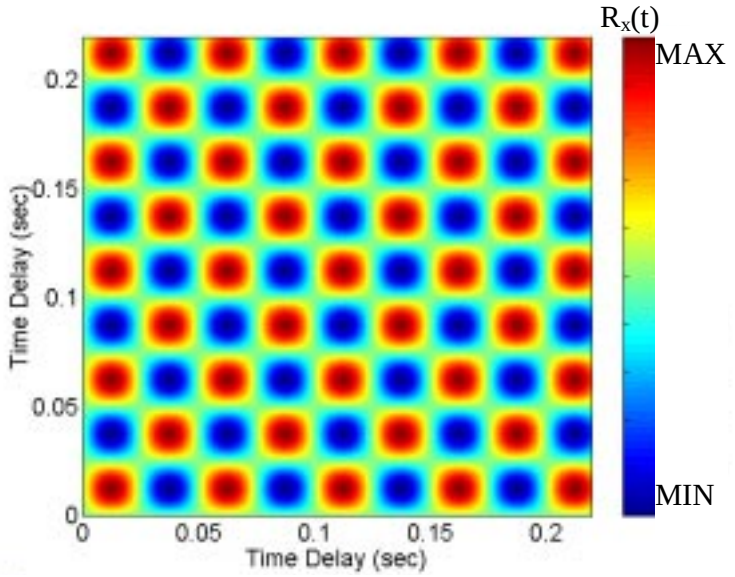

(a) Two-dimensional autocorrelation

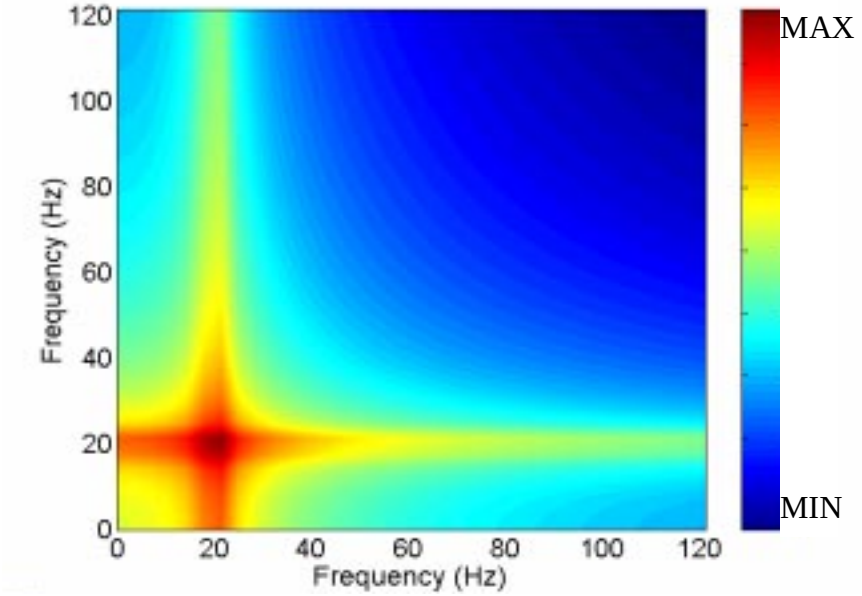

(b) Amplitude of two dimensional power density spectrum

Figure 6. Pure tone at 20 Hz.

Figure 7 shows the time history of the signal up to 0.25 sec, which has a period of 0.05 sec. Figure 8 shows the one-dimensional spectrum of the signal, in which all 20 tones (fundamental plus 19 harmonics) can be observed. This particular example resembles the signal from a helicopter without a tail rotor, such as the MD 902 Explorer.

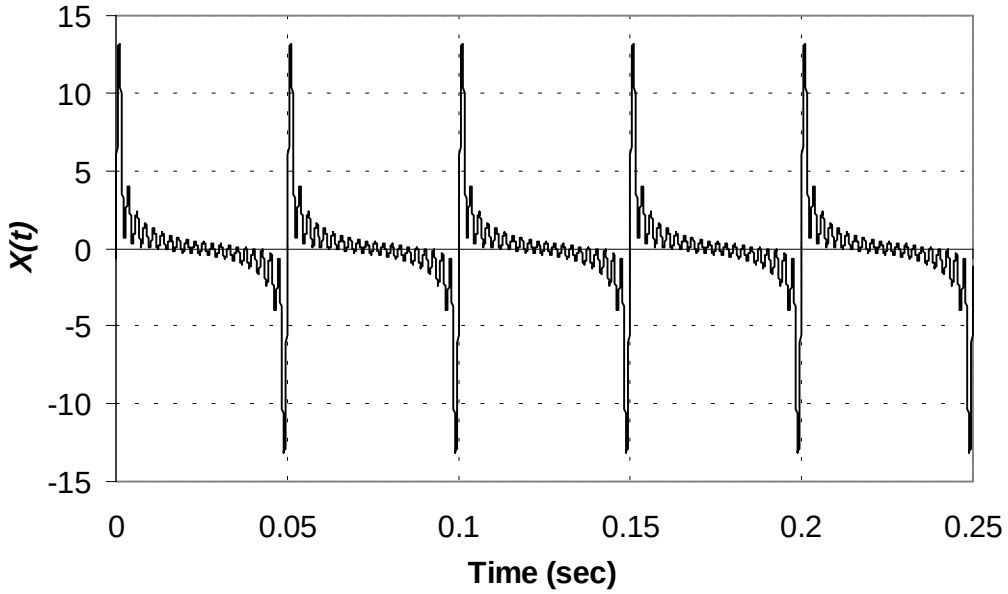

Figure 7. Time history of periodically correlated signal.

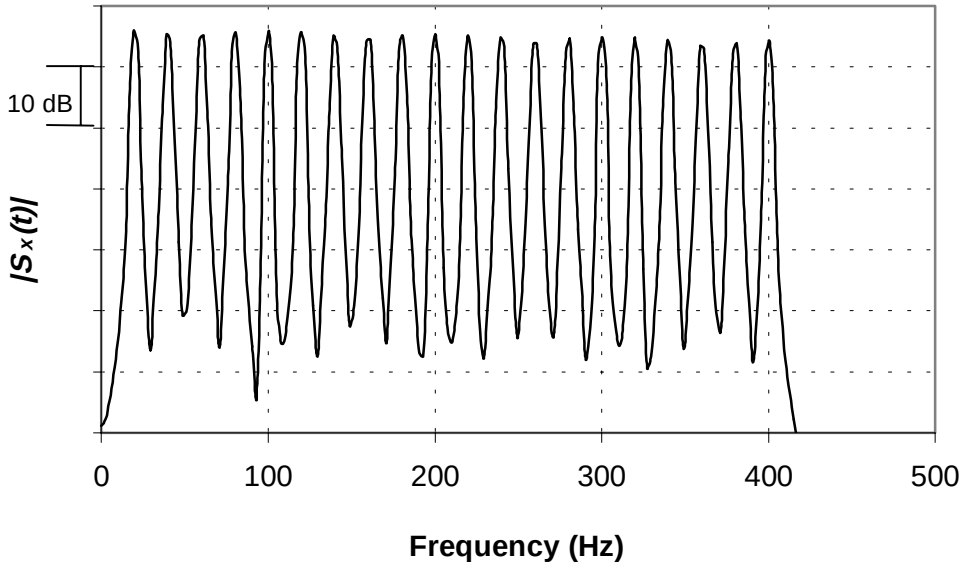

Figure 8. One dimensional power spectral density of periodically correlated signal.

Figure 9 shows the two-dimensional autocorrelation and power spectral density of the periodically correlated signal. Figure 9(a) shows a matrix of dots, which are equally

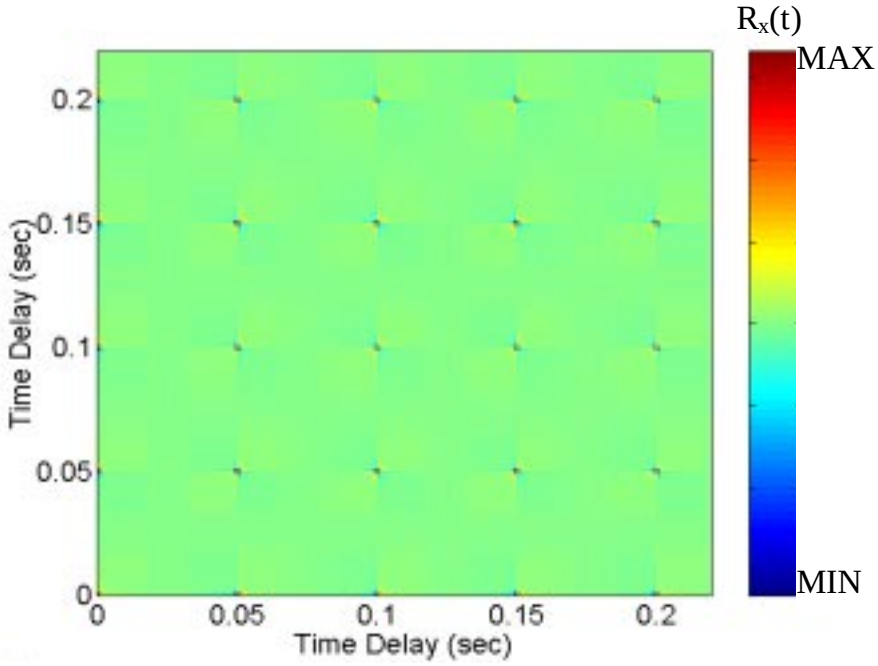

(a) Two-dimensional autocorrelation, Rx(t)

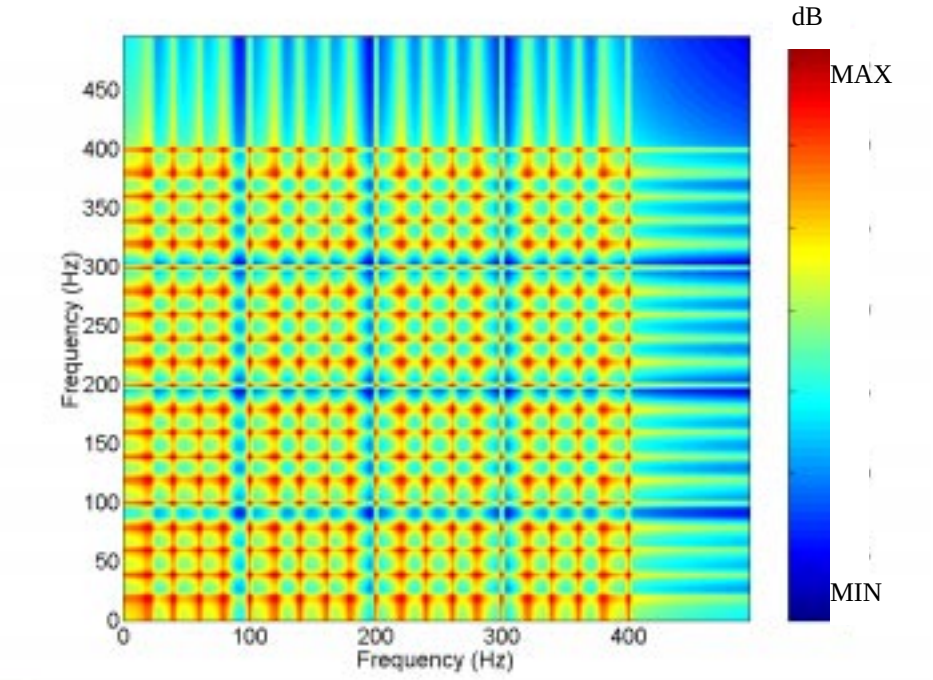

(b) Two dimensional power spectral density

Figure 9. Periodically correlated signal.

spaced by the period. The "support" lines described in [3] may be drawn in Fig. 9(b) by following the red "peaks" parallel to the diagonal, as these peaks are equally spaced.

Incommensurate Frequencies

To simulate a helicopter with a tail rotor, two sinusoidal signals with incommensurate frequencies are summed using the following equation:

$$X(t) = \sum_{i}^{20} (1 - 0.01i) \sin(2\pi 20it) + \sum_{j}^{2} (1 - 0.01j) \sin(2\pi 110jt) \qquad (13)$$

where t = 0 to 409.4 msec in increments of 0.2 msec.

The two frequencies differ by a factor of 5.5 (20 and 110 Hz), which is the main rotor-tail rotor ratio of the Sikorsky S-76C helicopter. The 20-Hz harmonics will be referred to as the main rotor tones and the 110-Hz harmonics will be called the tail rotor tones. The simulated signal includes harmonics with decreasing amplitude for both sinusoids. The time history of this signal is shown in Fig. 10. Though it appears periodic

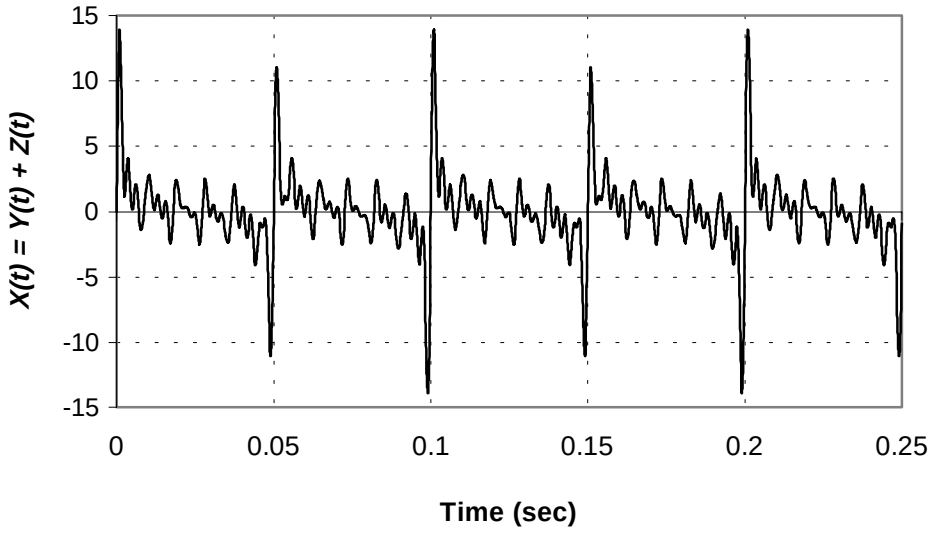

Figure 10. Time history of sum of periodic signals with incommensurate frequencies.

in nature, it is in fact non-periodic, as explained in Chapter 3. Figure 11 shows the one-dimensional spectrum of this non-periodic signal. Note the higher amplitude at 220 Hz,

where the 11th and 2nd harmonics, respectively, of the two signals are integer multiples of each other.

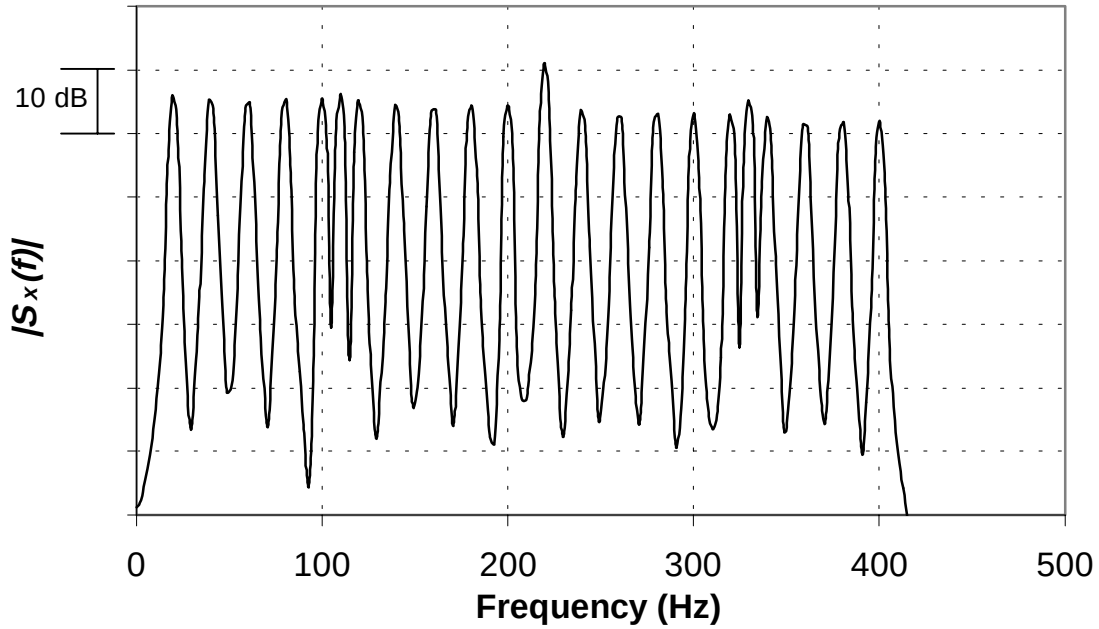

Figure 11. One dimensional power density spectrum of sum of periodic signals with incommensurate frequencies.

Figure 12 shows the two-dimensional autocorrelation and spectrum of the simulated non-periodic signal. Close observation of Fig. 12(a) reveals the peaks of the lower (main rotor frequency) represented as dots, and faint dots mark the higher (tail rotor) frequency. Fig. 12(b) shows all the frequencies generated in red, including the higher (tail rotor) frequency at multiples of 20 and 110 Hz.

Two diagonals, the center and tail rotor are marked on the two-dimensional spectrum in Fig. 12(b). The center diagonal is equivalent to the one-dimensional spectrum and contains information from all the frequencies in the signal. The tail rotor diagonal would only contain information from the tail rotor frequency at 110 Hz. The tail rotor diagonal is parallel to the center diagonal and offset by 110 Hz.

Figure 13 shows the center and tail rotor diagonals plotted together. The main rotor or 20 Hz tones were reduced significantly in the tail rotor diagonal. The fundamental and third harmonics of the tail rotor at 110 and 330 Hz, respectively, have retained their

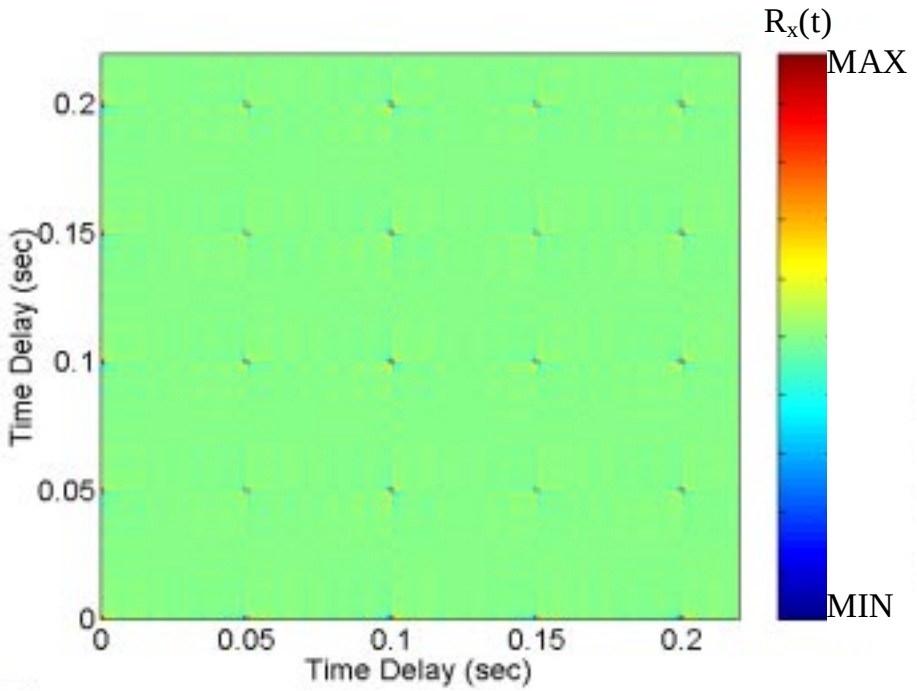

(a) Two-dimensional autocorrelation

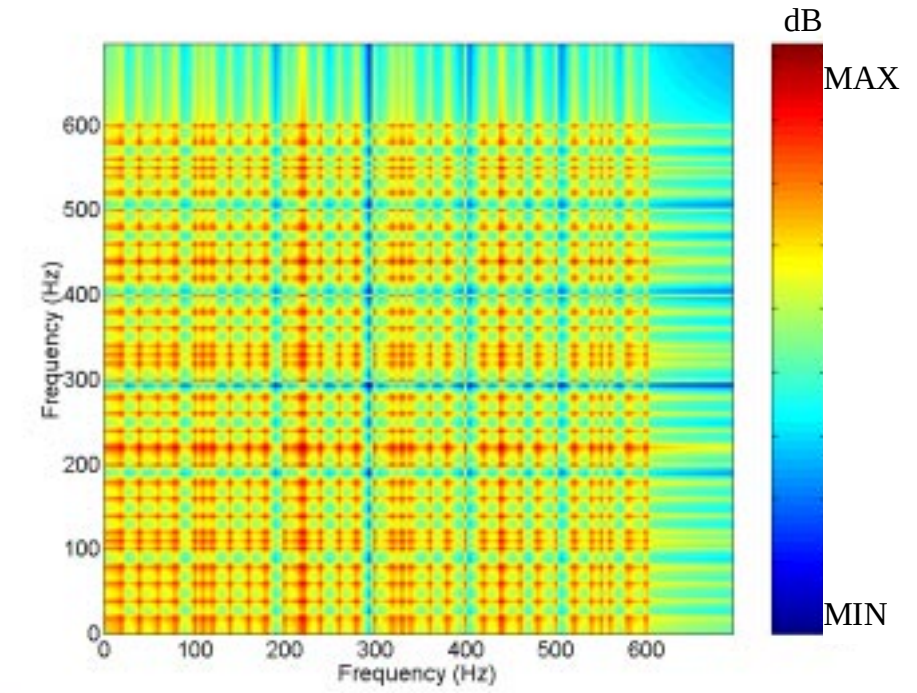

(b) Two-dimensional spectrum

Figure 12. Sum of periodic signals with incommensurate frequencies.

amplitude in the tail rotor diagonal. The second and fourth harmonics of the tail rotor at 220 and 440 Hz, respectively, are reduced by an average of 4 dB. Because the tones at 220 and 440 Hz are harmonics of both the main rotor and the tail rotor, the reductions in the tail rotor diagonal denote removal of the contribution of the main rotor to those tones.

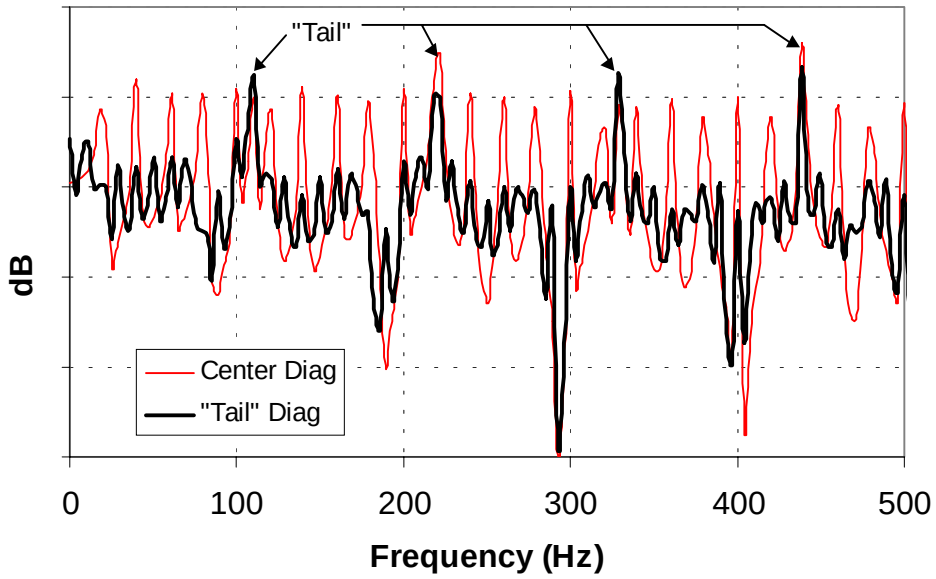

Figure 13. Center and “tail” diagonal from two-dimensional spectrum of sum of incommensurate frequencies.

In the next chapter, a flight test of two helicopters, one with a tail rotor and one without, will be described. Data from level flyovers of these two helicopters will be analyzed using the two-dimensional Fourier transform in Chapter 5. The two-dimensional Fourier transform spectra will be compared for the two aircraft in level flight, to assess the advantage of using the two-dimensional Fourier transform on an aircraft with a tail rotor. The two-dimensional Fourier transform for the helicopter with a tail rotor will then be presented for takeoff and approach conditions, to see variations in the two-dimensional spectra for different flight conditions.

CHAPTER 4

FLIGHT TEST DESCRIPTION

The experimental data used in this paper were acquired during the 1996 Noise Abatement Flight Test sponsored by the National Rotorcraft Technology Center (NRTC) and the Rotorcraft Industry Technology Association (RITA). Participating organizations were NASA Langley and Ames Research Centers, Volpe National Transportation Systems Center (Department of Transportation), Boeing Mesa (formerly McDonnell Douglas Helicopter Systems), and Sikorsky Aircraft. The test was conducted at the NASA Ames Crows Landing Flight Test Facility in Crows Landing, California.

The purpose of the test was to validate the Differential Global Positioning System (DGPS) for precision guidance for acoustic flight testing, with the specific application of designing high precision quieter approaches. For the purpose of this thesis, the flight test parameters provided an extensive database of helicopter flyovers for main rotor-tail rotor interaction analysis. Reference [13] describes the purpose and methodology of the flight test in depth.

Test Aircraft

Among the aircraft tested were a Boeing MD902 Explorer, and a Sikorsky S-76C+. The Boeing MD902 Explorer, shown in Fig. 14, is a five-bladed, eight-passenger helicopter featuring the NOTAR® anti-torque system (no tail rotor). Its rotor diameter is 33.83 ft, and its maximum takeoff gross weight (MTOGW) is 6250 lbs. Reference [14] describes the Boeing Explorer portion of the flight test.

Figure 15 shows the Sikorsky S-76C+ test aircraft. It is a 4-bladed (44-ft diameter), 10-passenger aircraft with a four-bladed tail rotor (8-ft diameter). Its gross takeoff weight during testing was nominally 11,200 lb, 500 lb less than its MTOGW of 11,700 lb. Reference [15] provides a description and results from the Sikorsky S-76C+ portion of the flight test.

Figure 14. Boeing MD902 Explorer.

Figure 15. Sikorsky S-76C+.

Microphone Layout

The test aircraft flew over a 50-microphone array laid out on agricultural land adjacent to the Crows Landing main runway. Figure 16 is a schematic of the array, which encompassed approximately 1.1 sq. mi. Data was acquired by four different groups: Sikorsky, Boeing Mesa, and Volpe using Sony digital DAT recorders, and NASA Langley using the field digital acquisition system. Microphones labeled N26, N27, and N28 in Fig. 16 are used in this paper. These were selected for their locations along the flight track, and ease of accessing the data. The data from these three microphones were recorded on the same tape by one of the NASA digital systems. They will be referred to

as the port (N26), centerline (N27), and starboard (N28) microphones hereafter in this thesis.

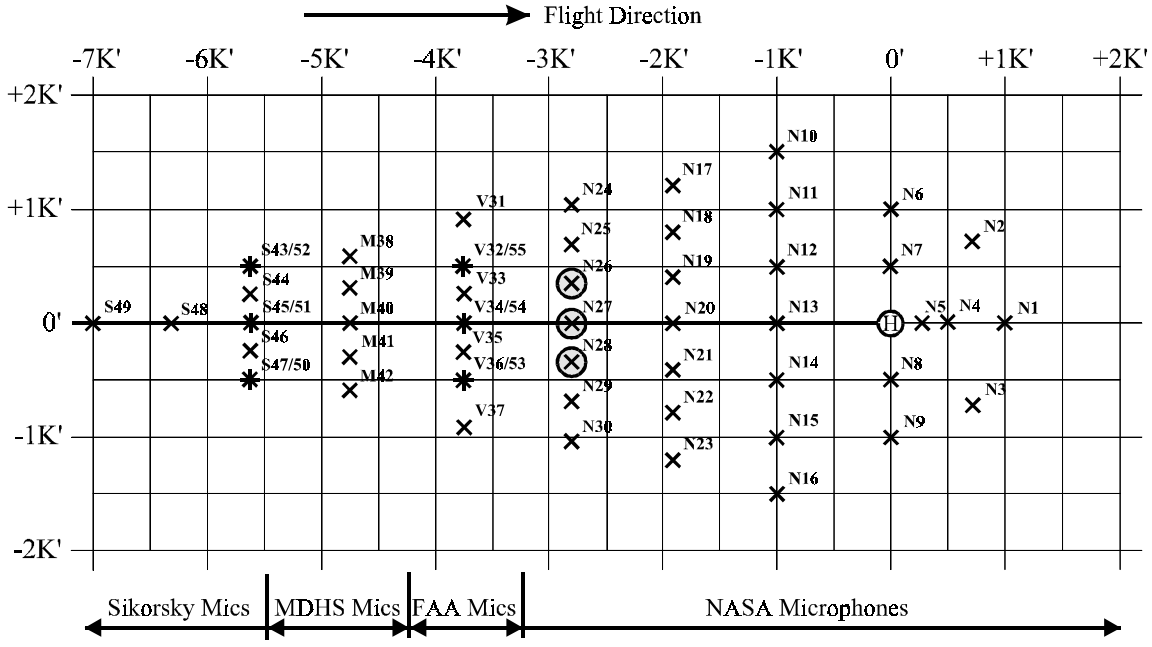

Figure 16. Microphone array layout at Crows Landing, CA, during flight test.

Flight Parameters

Approaches were flown to a hover over the hover pad, with glideslopes such that the aircraft was at 394 ft altitude when over the reference microphone. Level flyovers were flown at various altitudes. For the S-76, departures began at a nominal 200 ft altitude and 394 ft directly overhead of the reference microphone. No departure or takeoff data was recorded for the MD 902 Explorer.

Data Acquisition and Analysis

Data for the three microphones presented in this paper were acquired at a 20 kHz sampling rate. Each data run varied in length, depending on the flight parameters such as glideslope, and speed. For the purposes of this thesis, the data used from each flyover were chosen after inspecting their spectrograms. Spectrograms were produced by taking an 8192-pt Fast Fourier Transform (FFT) every 4096-pts of the signal for a 50% overlap. Figure 17 is an example of a spectrogram of a flyover. The horizontal axis in Fig. 17 denotes time, the vertical axis denotes frequency, and the sound pressure level (SPL) in

decibels (dB) is denoted by color. The main rotor tones are seen in Fig. 17 as the horizontal red lines beginning at about 40 Hz, and spaced about 40 Hz apart. The Doppler shift is seen as the shift in frequency of these main rotor tone lines. The frequency shift is especially severe near the overhead point at approximately 19 seconds into the flyover. Beyond the overhead point, some tones at approximately 200 Hz appear as orange-and-yellow lines at intervals of about 180 Hz. These tones, apparently radiated aft of the helicopter, since they are not very strong prior to the overhead point. Due to the proprietary nature of the acoustic data, no absolute dB levels are shown in this thesis. Data segments with high tone levels and low Doppler shift have been selected as the best to represent the noise of the flyover.

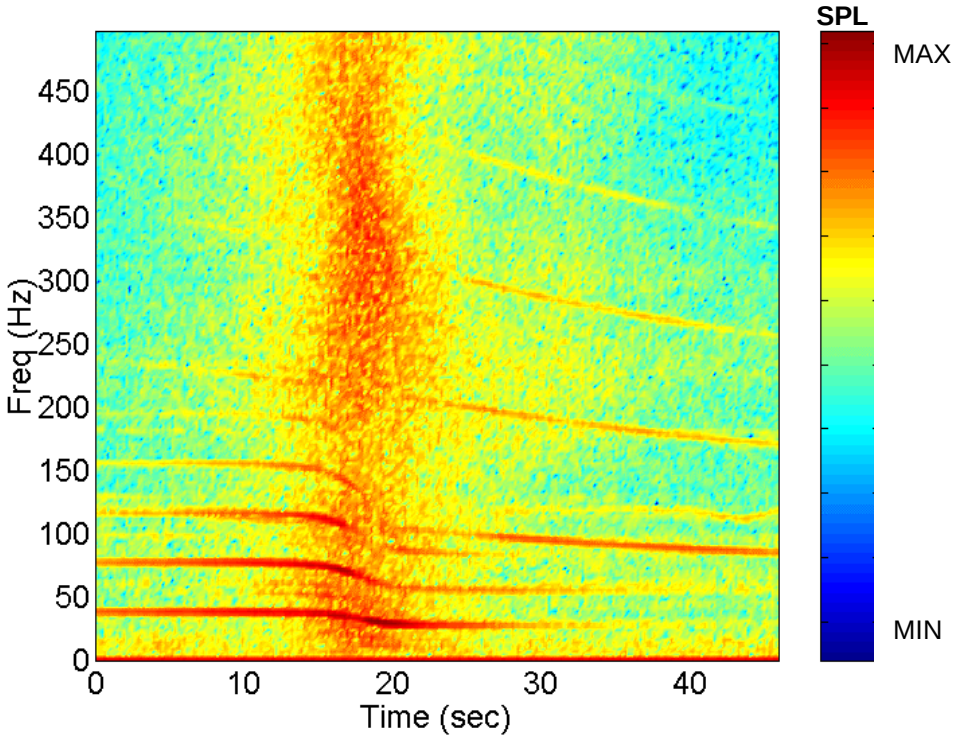

Figure 17. Spectrogram of Boeing MD902 Explorer level flyover recorded by centerline microphone.

CHAPTER 5

RESULTS WITH EXPERIMENTAL DATA

The time histories of selected runs from the 1996 Crows Landing flight test have been analyzed using MATLAB software. The first step is to identify, as described in Chap. 4, a suitable "slice" of data from each selected run. A starting point is then identified in the signal. From this starting point, a segment with a length of an integer multiple of the main rotor is analyzed.

Table 1 lists the aircraft distances relative to the three microphones used for the start and end of the data segments used in the Fourier analyses. The last column of Table 1 shows the distance traveled by the aircraft during the data set analyzed.

TABLE I
Aircraft Distances from Microphones

	Start Distance (ft) from			End Distance (ft) from			Travel
	Port	Centerline	Starboard	Port	Centerline	Starboard	Dist. (ft)
MD 902 Level	3252	3235	3255	3205	3187	3207	48
S-76C+ Level	3257	3238	3256	3182	3161	3180	77
S-76C+ Takeoff	1592	1546	1579	1562	1515	1548	45
S-76C+ Approach	3285	3267	3287	3244	3226	3247	41

One Dimensional Spectra

Boeing MD 902 Explorer

Figure 18 shows the one-dimensional spectra of a portion of a Boeing MD 902 Explorer level flyover for the three microphones specified in Chapter 4. As listed in Table 1, the aircraft was approximately 3200 ft away The spectra of Fig. 18 show that the

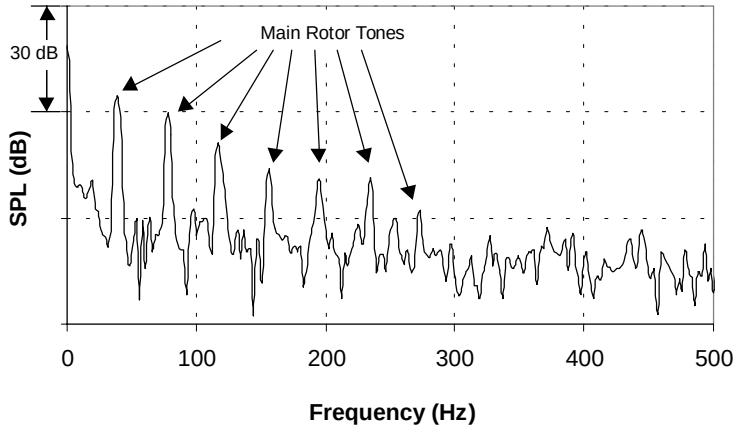

(a) Port Microphone (Retreating Side)

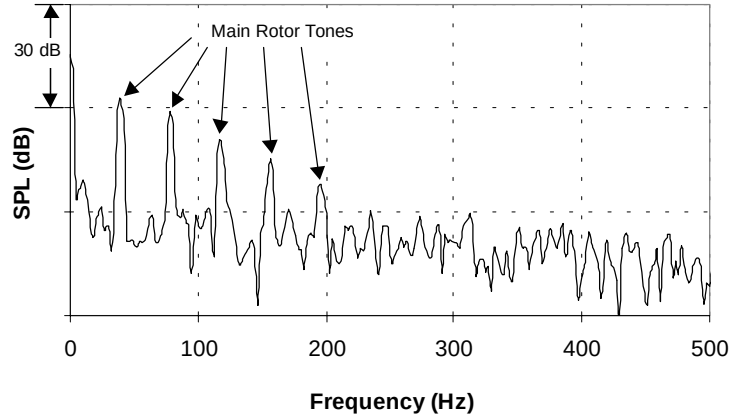

(b) Centerline Microphone

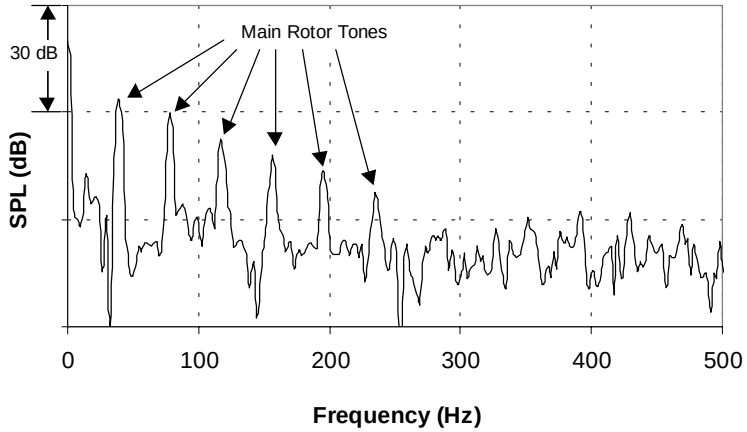

(c) Starboard Microphone (Advancing Side)

Figure 18. Boeing MD902 Explorer spectra for level flyover at 115 knots, 500 ft altitude.

noise measured by these microphones was dominated by the main rotor harmonics. The fundamental BPF tones at 39 Hz for all three microphones was about 30 dB above the noise floor. Six harmonics were at least 10 dB above the noise floor from the port and starboard microphones, and 5 harmonics from the centerline microphone. Disregarding the other discernible tones with comparatively low sound pressure level (SPL), the signals whose spectra were shown in Fig. 18 would be considered periodic. Therefore, the one-dimensional spectrum should be sufficient to describe the spectral characteristics of this aircraft.

Sikorsky S-76C+ - Level Flight

Figure 19 shows the spectra from a Sikorsky S-76C+ level flyover for the three microphones. As with the Boeing MD 902 Explorer, the Sikorsky S-76C+ was approximately 3200 ft away from the microphones during the data segment shown. The main rotor tones, beginning at 25 Hz, are dominant in the signals from the centerline and starboard microphones, with the 4^{th} and 5^{th} harmonic showing the highest levels in the spectra. For the port side microphone, the 5^{th} harmonic exhibits the highest level in the spectrum.

The tail rotor fundamental BPF was 141 Hz. Although 10 – 20 dB lower than the highest levels in the three spectra, the tail rotor tones are discernible and are labeled in Fig. 19. Note that the tail rotor tone at approximately 280 Hz was also a multiple of the main rotor BPF, therefore there was some energy from the main rotor noise in this particular tone.

Sikorsky S-76C+ - Takeoff

Figure 20 shows the one-dimensional spectra from the three microphones for a Sikorsky S-76C+ takeoff. Table 1 lists the distance from the microphones as approximately 1500 ft. As mentioned in Chapter 3, reference [7] indicated a stronger tail rotor signal during takeoff. Indeed, the tail rotor tones are very dominant in the spectra of Fig. 20. The third harmonic of the main rotor BPF for all three spectra in Fig. 20 appears "smeared," especially in comparison to the first and second harmonics.

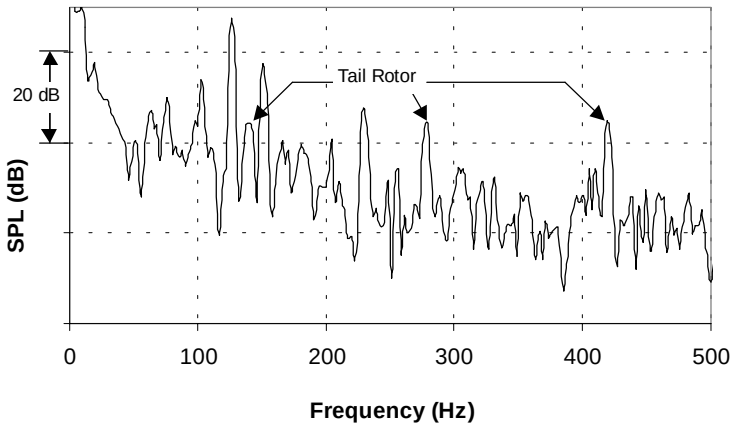

(a) Port Microphone (Retreating Side)

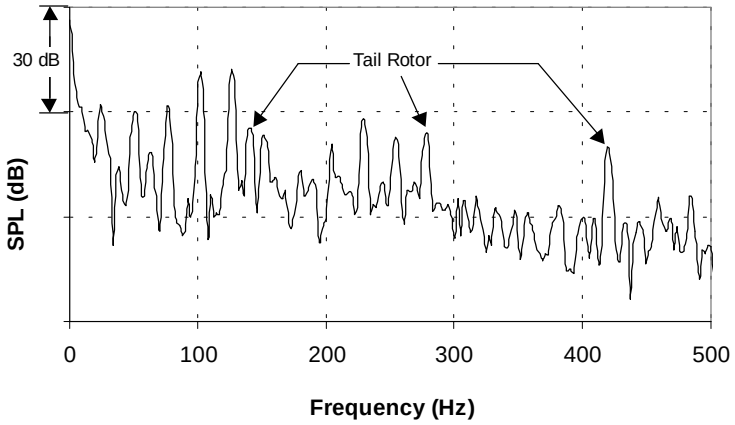

(b) Centerline Microphone

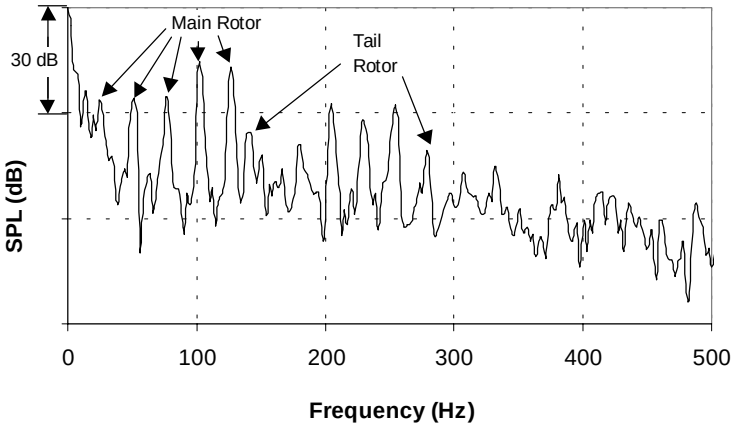

(c) Starboard Microphone (Advancing Side)

Figure 19. Sikorsky S-76C+ level flyover at 136 knots, 492 ft altitude.

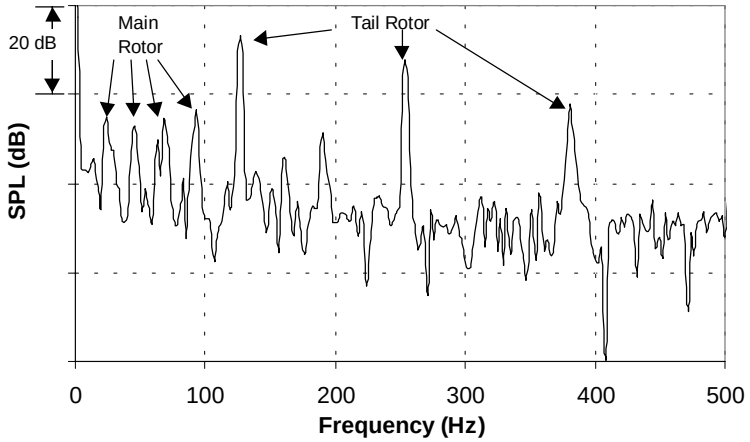

(a) Port Microphone (Retreating Side)

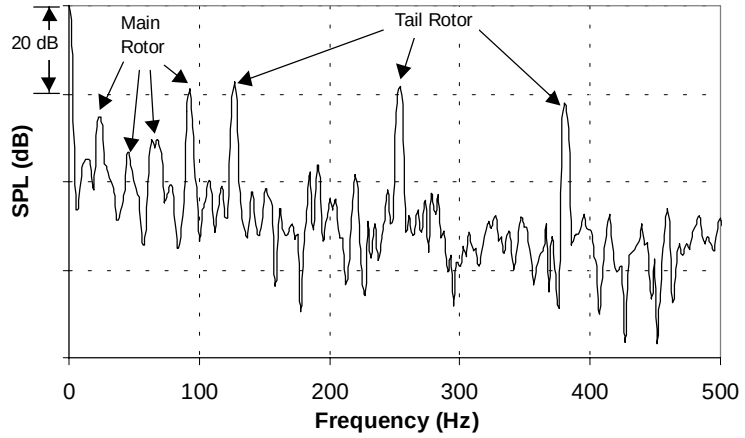

(b) Centerline Microphone

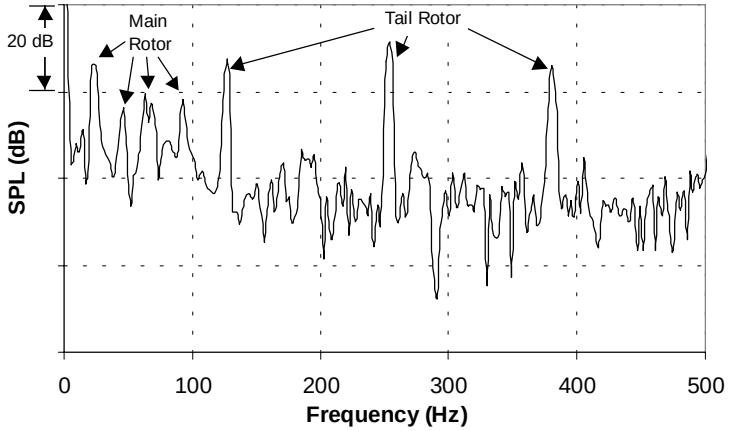

(c) Starboard Microphone (Advancing Side)

Figure 20. Sikorsky S-76C+ takeoff at 74 knots.

Sikorsky S-76C+ - Approach

Figure 21 shows the one-dimensional spectra for the three microphones for a 6-deg, 74 kt approach of the Sikorsky S-76C+. Helicopter approach noise is typically dominated by blade-vortex interaction noise (BVI) as the main rotor blade tip vortices intersect with the main rotor blades in descent. The three spectra in Fig. 21 indeed show sharp peaks for almost every multiple of the main rotor BPF up to 500 Hz. These peaks rise approximately 10 to 20 dB above the noise floor. The tail rotor BPF can be identified, but because the fundamental and third harmonics of the tail rotor BPF are so close to the main rotor harmonics, the peaks are not as distinct at those of the main rotor harmonics. It can also be observed that the sound pressure levels are lower for the centerline microphone, especially at the tail rotor frequency.

Two Dimensional Spectra

Boeing MD902 Explorer – Level Flight

Figure 22 shows the two-dimensional autocorrelations and power spectra for the three microphones for a Boeing MD 902 level flight. The autocorrelations and spectra are calculated from one block of data. Appendix B lists the MATLAB script used to calculate these matrices. The block length is equal to ten main rotor blade passage periods. The number of periods is chosen to maximize the number of periods processed without encountering computer memory problems. The signal is resampled at a rate of 5 kHz, resulting in a spectral bandwidth of approximately 4 Hz. Figures 22 (a), (b), and (c) show the autocorrelations of the signal that exhibit the periodic peaks of the main rotor harmonics, similar to that of the simulated signal shown in Fig. 9(a). Figures 22 (b), (d), and (f) show the spectra that exhibit a similar pattern as the simulated signal spectrum in Fig. 9(b), but with less power in the harmonics above the third.

Diagonals are superimposed on the spectra in Figures 22 (a), (b), and (c): one represents the center or main diagonal of the spectrum, and the other cuts through the fundamental BPF of the main rotor. The center diagonals and the fundamental BPF diagonals for the three microphones are plotted in Fig. 23.

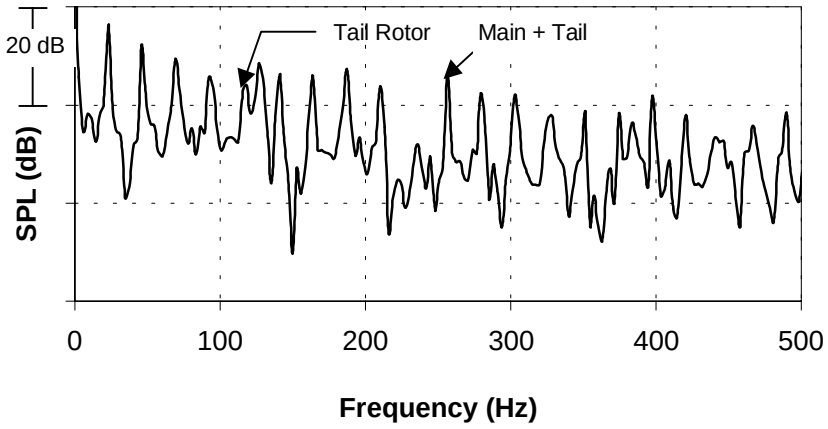

(a) Port microphone (retreating side)

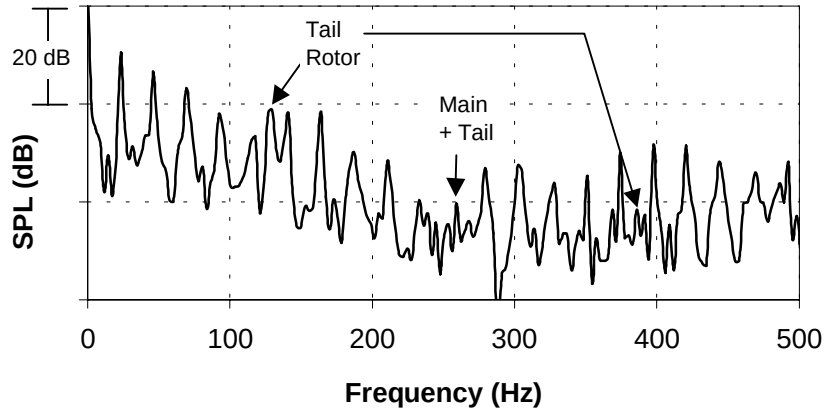

(b) Centerline microphone

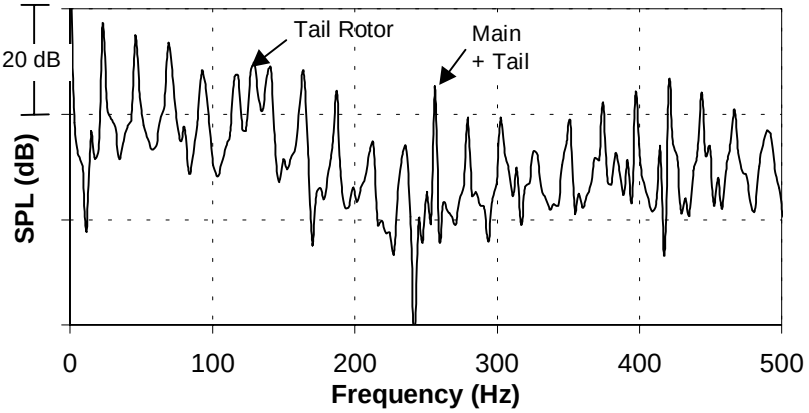

(c) Starboard microphone (advancing side)

Figure 21. Sikorsky S-76C+ 6-deg approach at 74 kts.

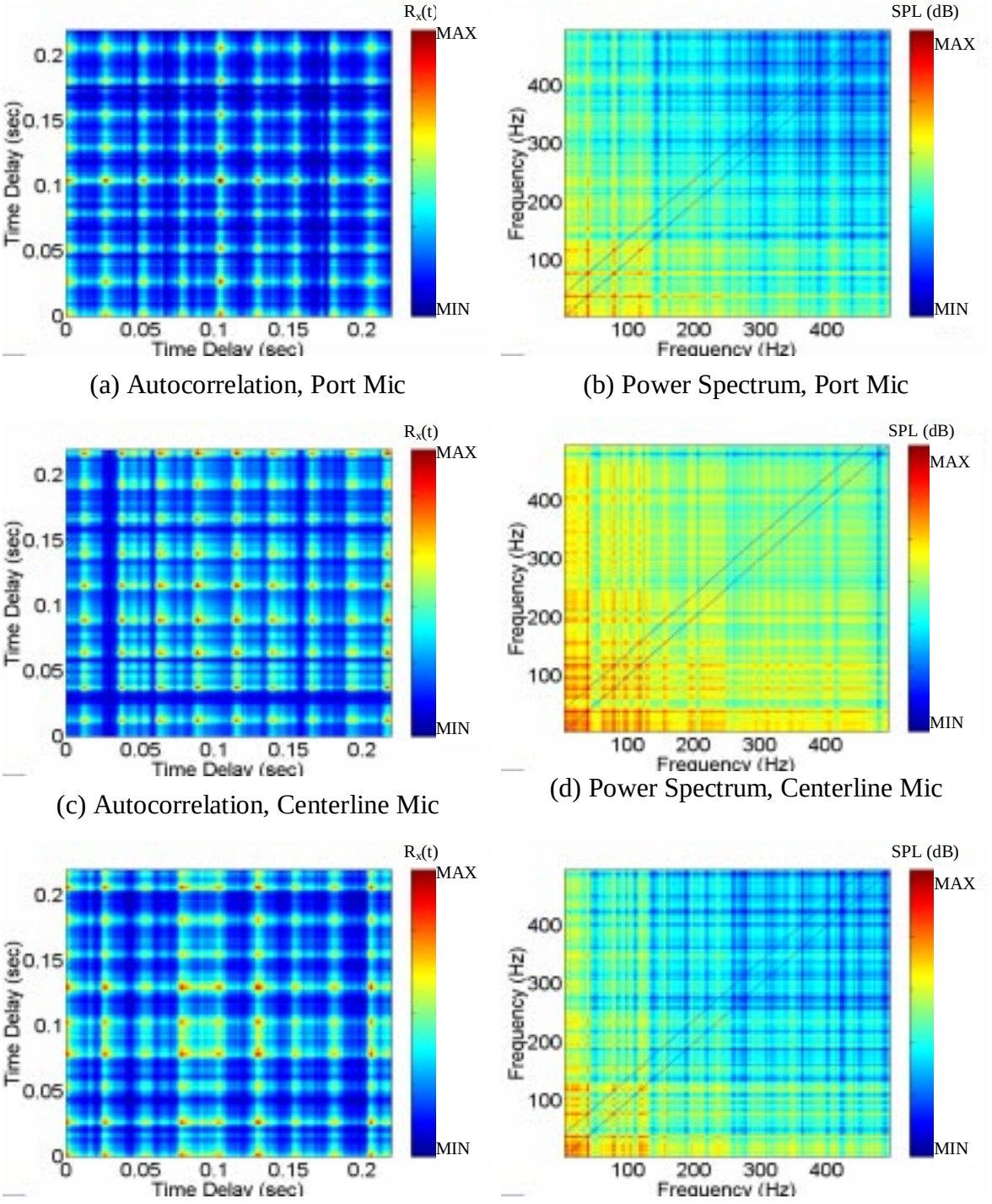

(a) Autocorrelation, Port Mic

(b) Power Spectrum, Port Mic

(c) Autocorrelation, Centerline Mic

(d) Power Spectrum, Centerline Mic

(e) Autocorrelation, Starboard Mic

(f) Power Spectrum, Starboard Mic

Figure 22. Boeing MD902 Explorer spectra for level flyover at 115 knots, 500 ft altitude.

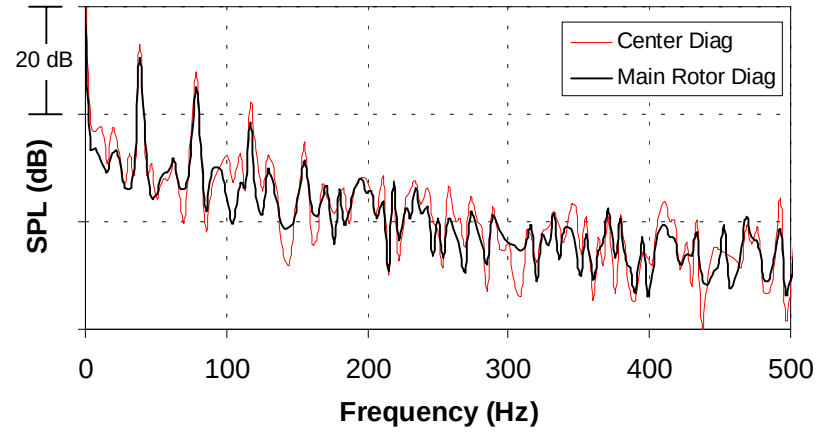

(a) Port Microphone (Retreating Side)

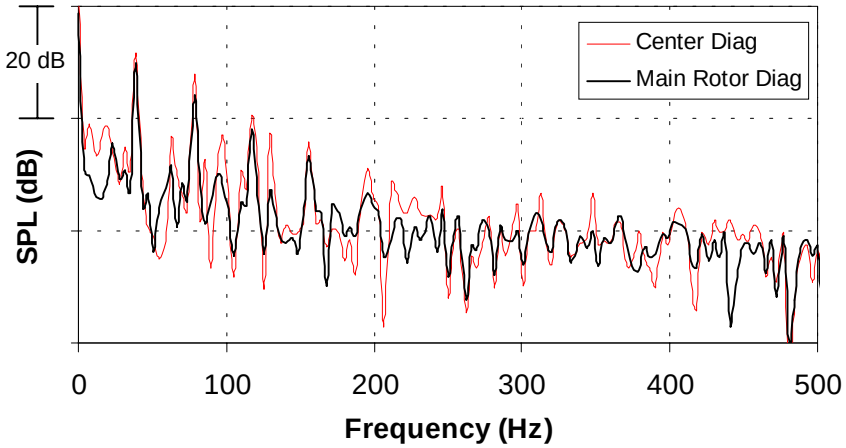

(b) Centerline Microphone

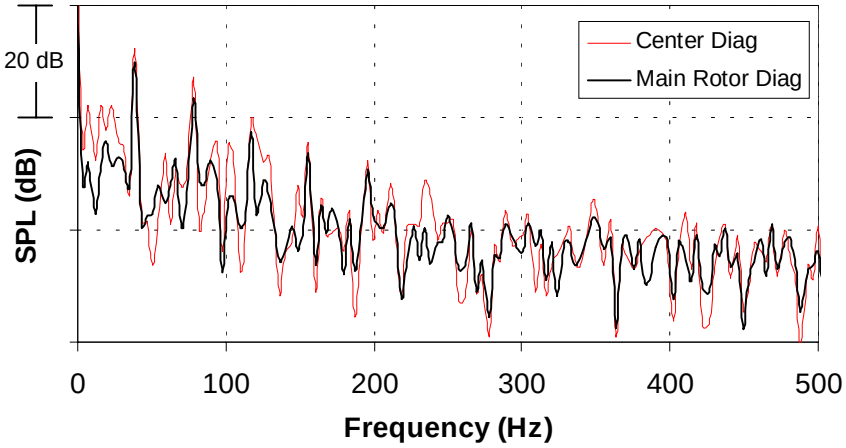

(c) Starboard Microphone (Advancing Side)

Figure 23. Boeing MD 902 level flyover, center and main rotor BPF diagonals from two-dimensional spectra.

The center diagonal of the two-dimensional spectrum is closely related to the one-dimensional Fourier transform of the signal. It contains information from all frequencies present in the signal. The main rotor diagonal, in theory, would give information only from the main rotor BPF and harmonics.

The main rotor diagonals (black lines) in Fig. 23 show a decrease in SPL of up to 14 dB for frequencies not associated with the main rotor BPF. For example, a tone around 130 Hz in Fig. 23(b) is reduced by 10 dB from the center to the main rotor diagonal. The main rotor harmonics up to 4 BPF maintained their SPL within 4 dB from the center diagonal. These observations indicate that the main rotor diagonal indeed contains information associated only with the main rotor BPF. This information could be useful in analysis of noise generated by the main rotor as it removes extraneous noise that gets added to the overall spectrum.

Sikorsky S-76C+ - Level Flight

Figure 24 shows the two-dimensional autocorrelation and power density spectra for a level flyover of the Sikorsky S-76C+. The autocorrelations and spectra are calculated using a block length containing ten periods of the main rotor blade passage. The difference in strength within the autocorrelation of Fig. 24(e) represent the variations in signal strength for each blade passage. The difference in strength between the three microphones could be attributed to the higher noise levels typically measured on the advancing (starboard) side of the aircraft. The spectra of Figs. 24 (b), (d), and (f) show higher SPL on the advancing side of the helicopter rotor.

The center, main rotor BPF and tail rotor BPF diagonals are marked on the spectra of Figs. 24 (b), (d), and (f). The center and main rotor diagonals are plotted together in Fig. 25, and the center and tail rotor diagonals are plotted together in Fig. 26.

The main rotor diagonals shown in Fig. 25 show a marked decrease in the SPL at the tail rotor frequencies. This decrease is to be especially noted in Fig. 25(c), the

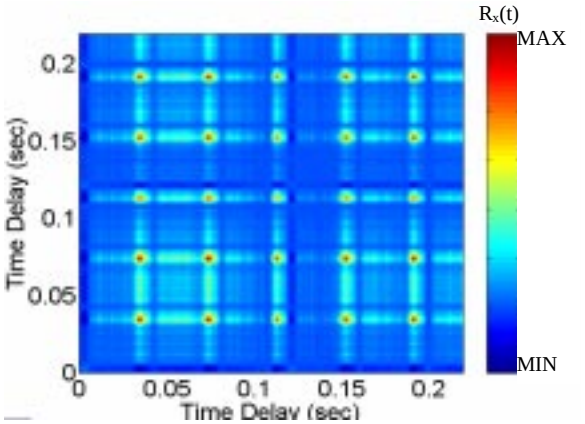

(a) Autocorrelation, Port Mic

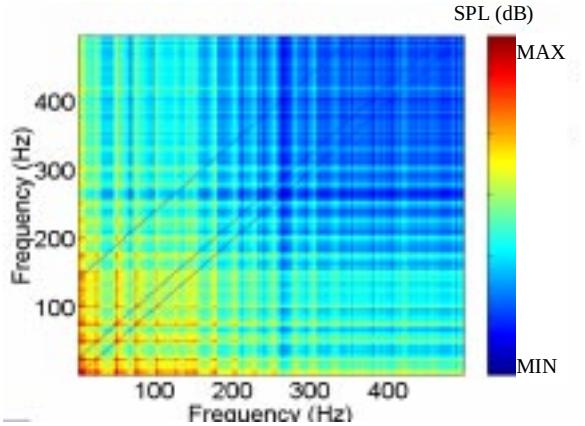

(b) Power Spectrum, Port Mic

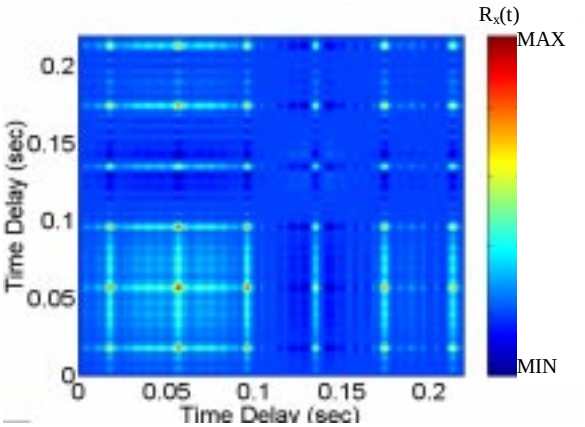

(c) Autocorrelation, Centerline Mic

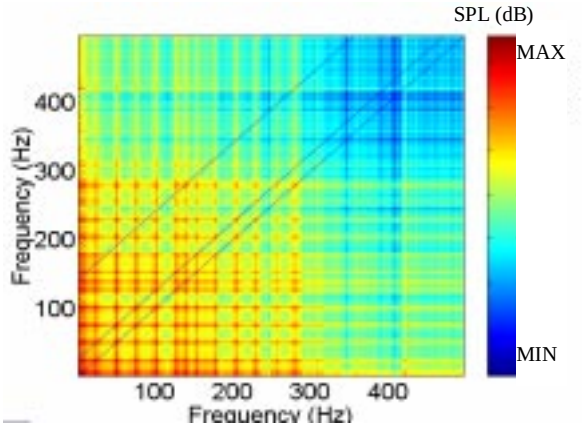

(d) Power Spectrum, Centerline Mic

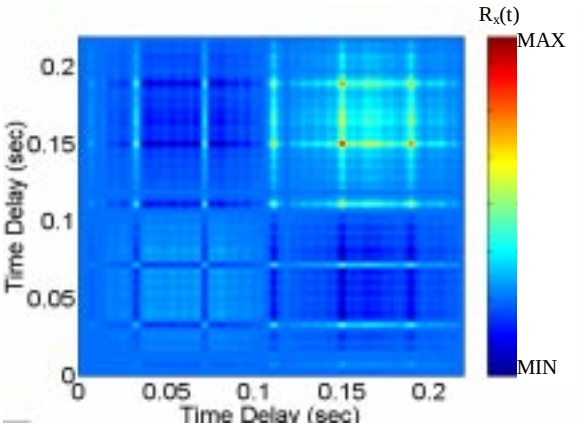

(e) Autocorrelation, Starboard Mic

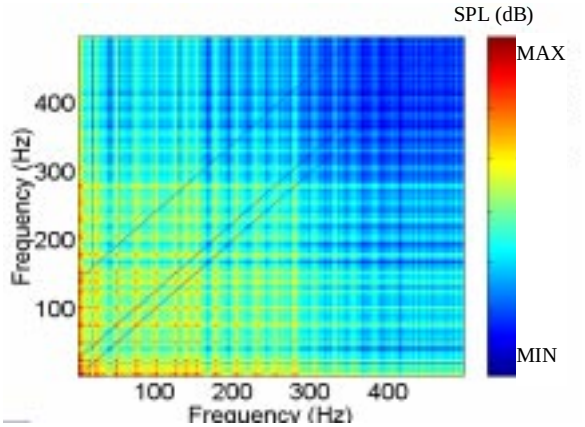

(f) Power Spectrum, Starboard Mic

Figure 24. Sikorsky S-76C+ level flyover at 136 knots, 492 ft altitude.

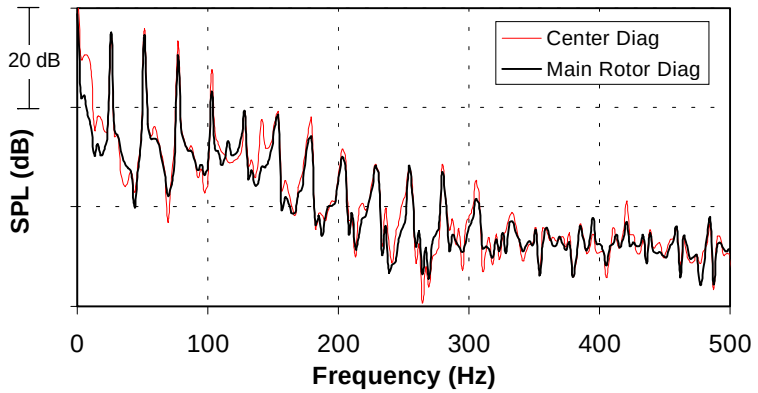

(a) Port Microphone (Retreating side)

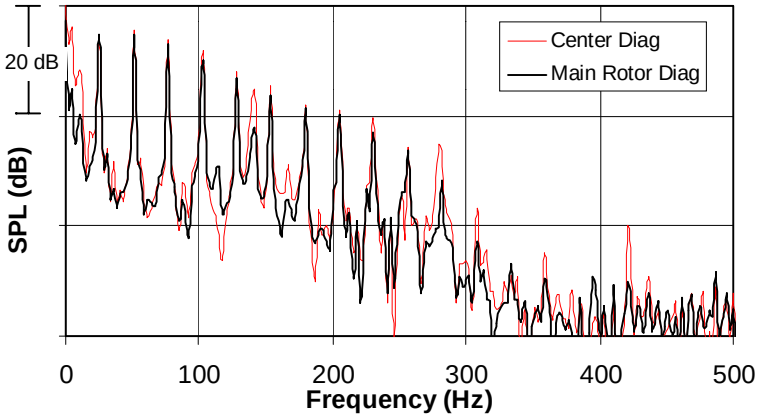

(b) Centerline Microphone

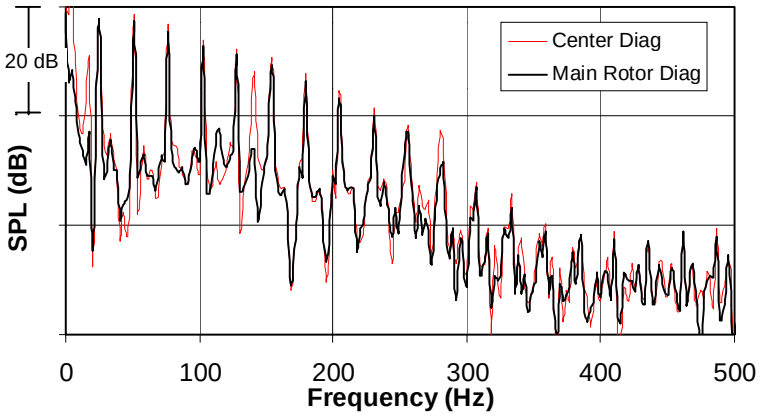

(c) Starboard Microphone (Advancing side)

Figure 25. Center and main rotor diagonals from two-dimensional spectra, Sikorsky S-76C+ level flyover at 136 kts.

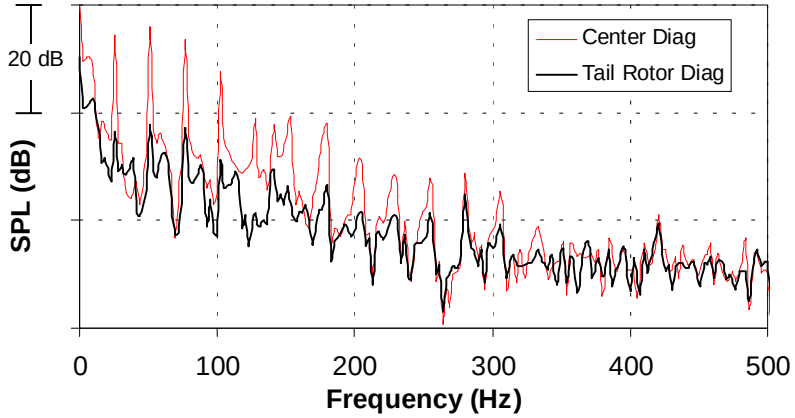

(a) Port microphone (Retreating side)

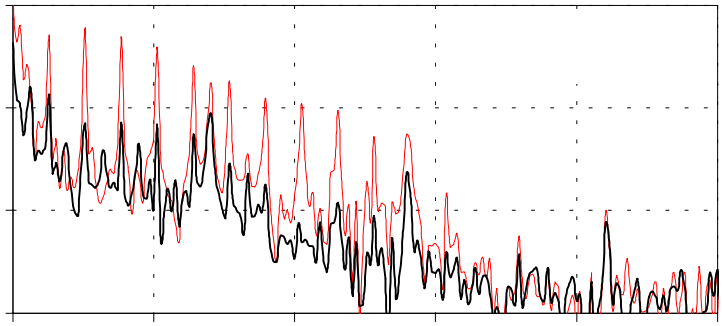

(b) Centerline microphone

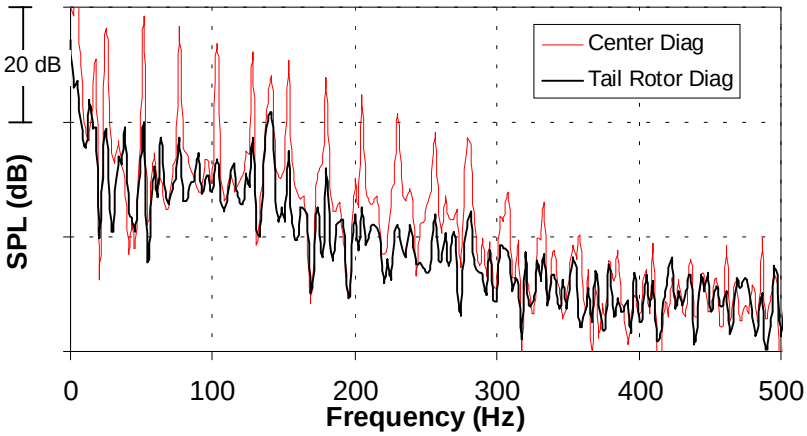

(c) Starboard Microphone (Advancing side)

Figure 26. Center and tail rotor diagonals from two-dimensional spectra, Sikorsky S-76C+ level flyover at 136 kts.

microphone located on the advancing side of the rotor, where the tail rotor BPF around 140 Hz decreases by almost 14 dB. Note that at 2BPF of the tail rotor, the reduction is not as great. This happens to be 11 BPF of the main rotor, therefore the remaining power should be the contribution of the main rotor at that frequency.

The diagonals shown in Fig. 26 show a dramatic decrease in SPL of the main rotor tones. The tail rotor diagonals should be representations of the noise contributions of the tail rotor to the overall spectra. The reduction in the tail rotor tones is thought to be related to main rotor-tail rotor interaction.

Sikorsky S-76C+ - Takeoff

The two-dimensional autocorrelations and power spectra for a Sikorsky S-76C+ are shown in Fig. 27. These are calculated using one data block, the length of which contains exactly eight periods of the main rotor blade passage. In the autocorrelations of Fig. 27, the main rotor peaks are evident, as are the tail rotor peaks, which appear as "tick marks" between the main rotor peaks. The spectra of Fig. 27 show the dominant tail rotor peaks, as seen in Fig. 20.

Diagonals going through the center, main rotor BPF, and tail rotor BPF are marked on the spectra of Fig. 27. The center and main rotor diagonals are shown superimposed in Fig. 28. Figure 28 shows that the tail rotor tones are greatly reduced, while the main rotor tones are diminished by 0 to 4 dB. This information may be useful in studying main rotor-tail rotor interaction noise, as some tones appear in the main rotor diagonals of Fig. 28. Specifically, around 230 Hz and 360 Hz, the main rotor diagonal intersects tones whose frequencies are related to both the main and tail rotor.

The center and tail rotor diagonals for the spectra of Fig. 27 are shown in Fig. 29. Main rotor tones are greatly reduced, while tail rotor tones maintain their amplitude very closely. There are no instances of tone generation such as those seen in Fig. 28 at 230 and 360 Hz in the tail rotor diagonals.

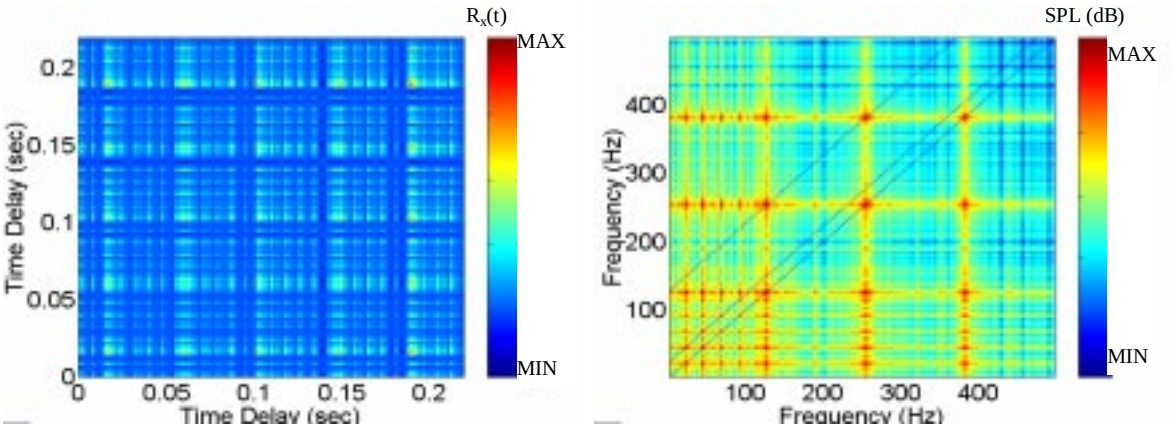

(a) Autocorrelation, Port Mic

(b) Port Microphone (Retreating Side)

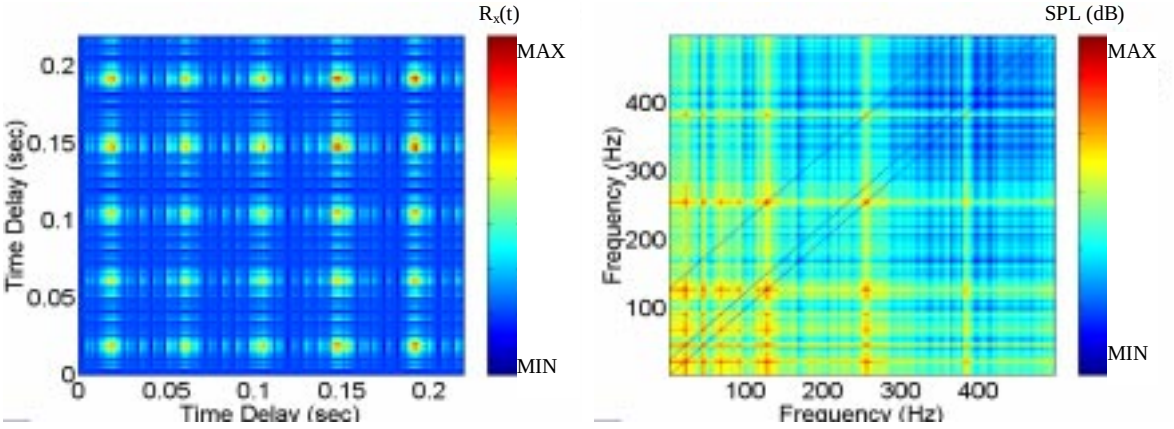

(c) Autocorrelation, Centerline Mic

(d) Power Spectrum Centerline Mic

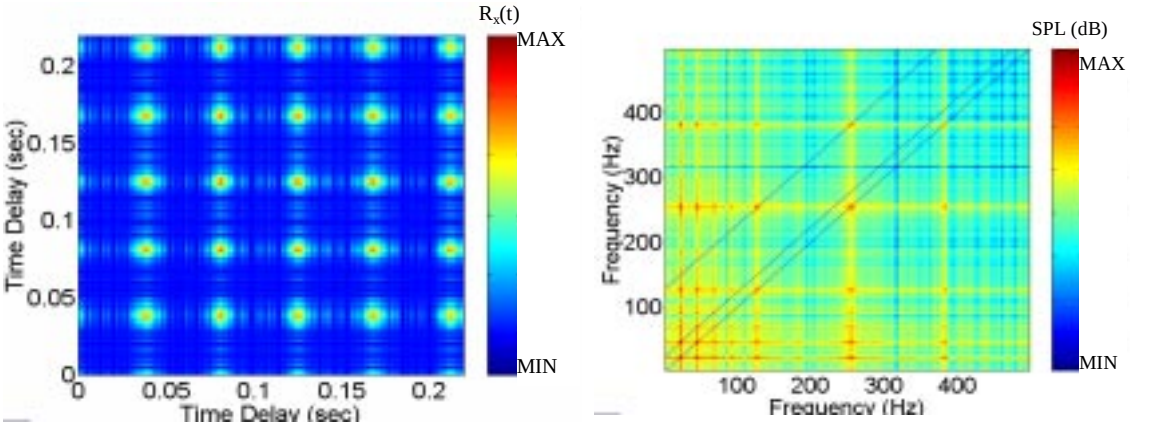

(e) Autocorrelation, Starboard Mic

(f) Power Spectrum, Starboard Mic

Figure 27. Sikorsky S-76C+ takeoff at 74 knots.

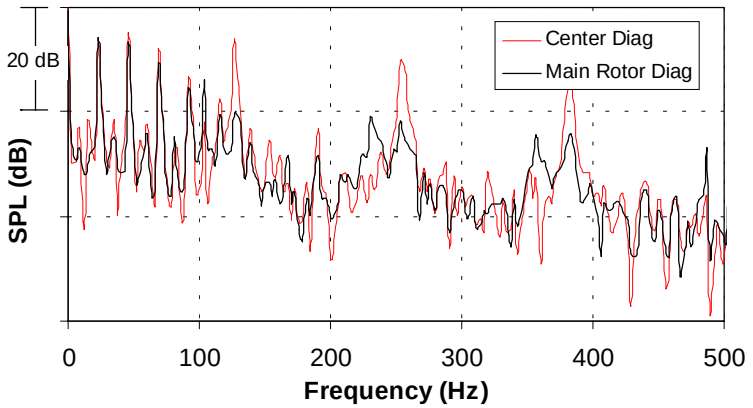

(a) Port Microphone (Retreating side)

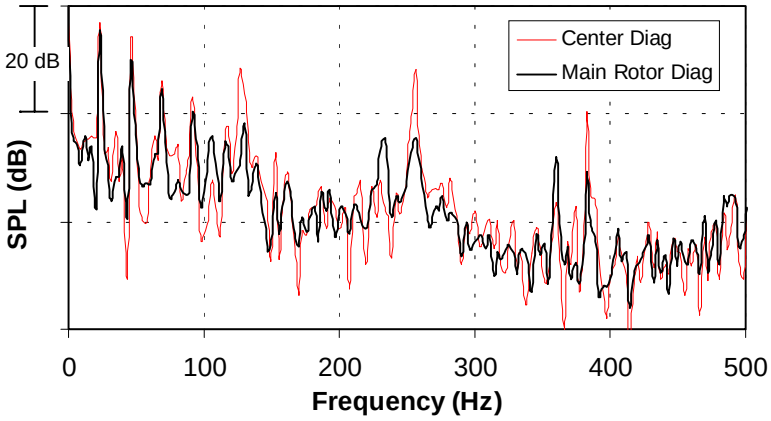

(b) Centerline Microphone

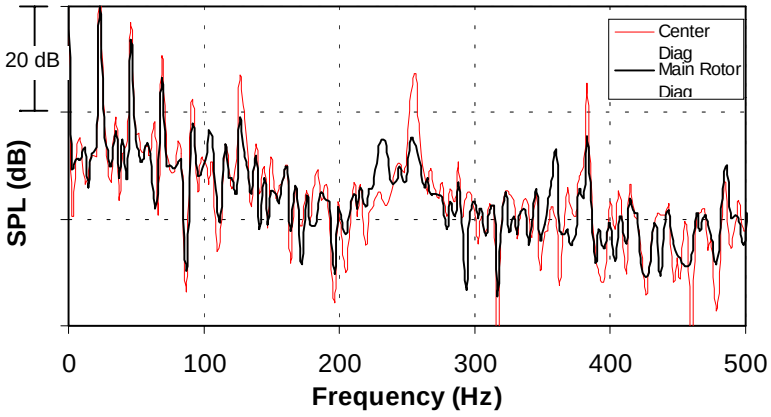

(c) Starboard Microphone (Advancing side)

Figure 28. Center and main rotor diagonals from two-dimensional spectra, Sikorsky S-76C+ takeoff at 74 knots.

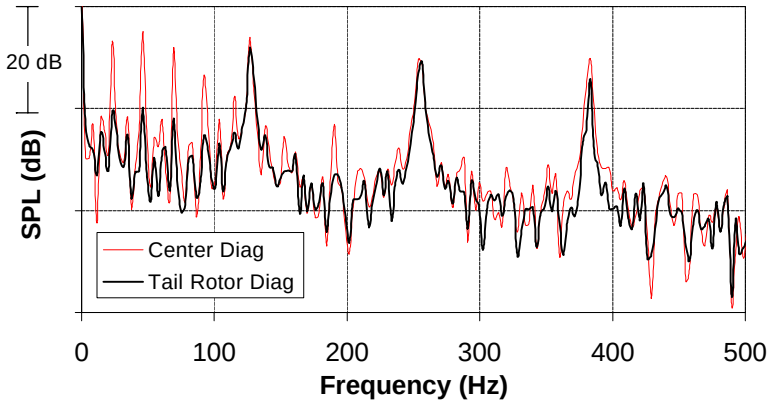

(a) Port Microphone (Retreating side)

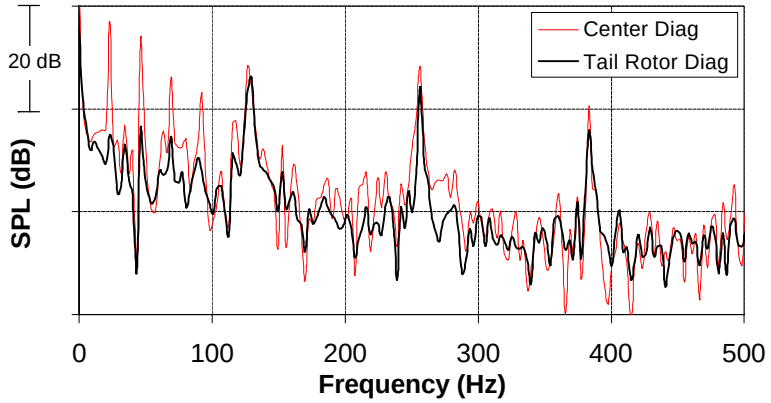

(b) Centerline Microphone

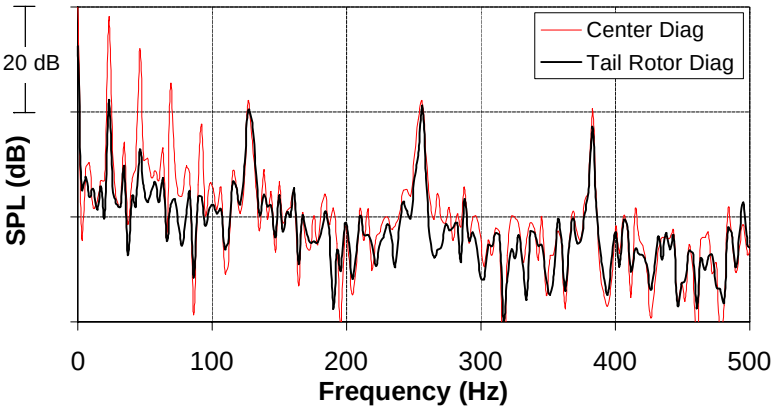

(c) Starboard Microphone (Advancing side)

Figure 29. Center and tail rotor diagonals from two-dimensional spectra, Sikorsky S-76C+ takeoff at 74 knots.

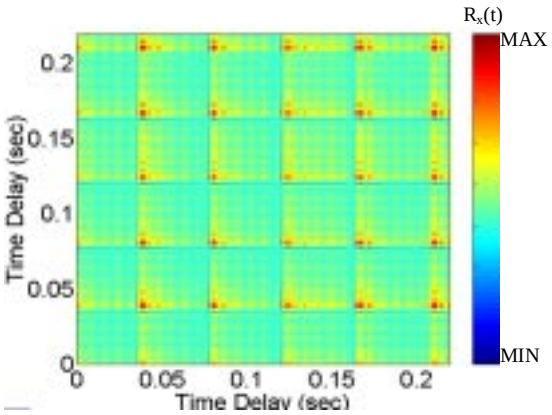

(a) Autocorrelation, Port Mic

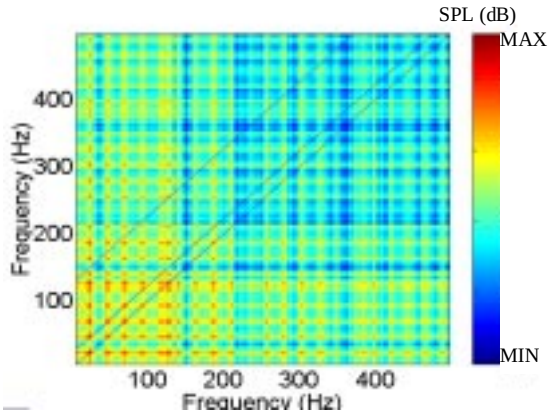

(b) Power Spectrum, Port Mic

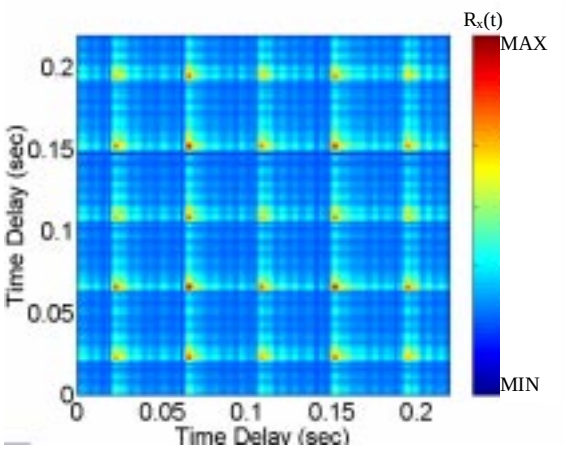

(c) Autocorrelation, Centerline Mic

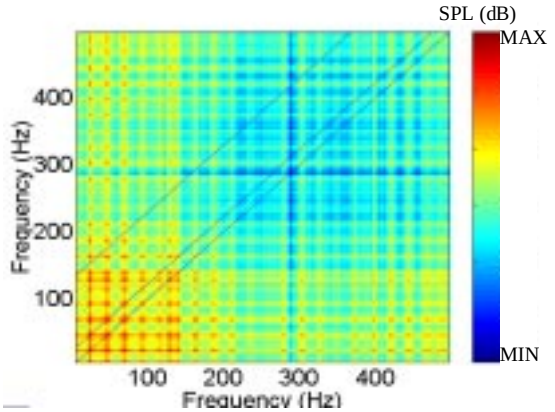

(d) Power Spectrum, Centerline Mic

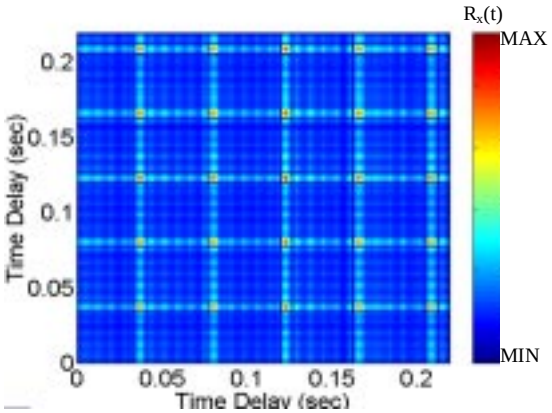

(e) Autocorrelation, Starboard Mic

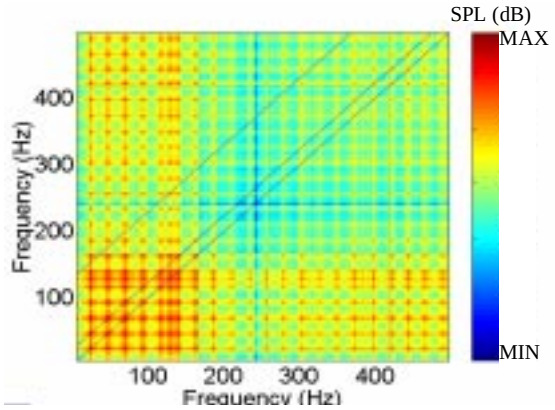

(f) Power Spectrum, Starboard Mic

Figure 30. Sikorsky S-76C+ 6-deg approach at 74 kts.

Sikorsky S-76C+ - Approach

The two-dimensional autocorrelations and spectra for the three microphones for a Sikorsky S-76C+ approach are shown in Fig. 30. The data block length used contains eight periods of the main rotor blade passage. The autocorrelations shown in Figs. 30 (a), (b), and (c) indicate a stronger signal in the starboard, or advancing side of the rotor. The spectra shown in Figs. 30 (b), (d), and (f) also reflect higher levels on the starboard side.

The superimposed center and main rotor diagonals are shown in Fig. 31. As expected, the main rotor tones are practically undiminished, while the first and third harmonics of the tail rotor are reduced considerably.

Approach noise is generally a main rotor-dominated signature, therefore looking for tail rotor noise during approach may be of interest. The center and tail rotor diagonals for the approach condition are shown in Fig. 32. The main rotor tones are reduced by about 10 dB for the first seven harmonics, while most of the tail rotor tones retain much of their amplitude. However, the centerline microphone shows a tail rotor diagonal with an amplitude approximately 15 dB lower than the main rotor diagonal. Referring to the one-dimensional spectrum of the centerline microphone in Fig. 21(b), it is obvious that the tail rotor BPF at 130 Hz has a strong presence in the spectrum. Unlike the port and starboard microphones, the 2BPF tail rotor tone is in the noise floor for the centerline microphone. This 2BPF tone is the first tone expected in the tail rotor diagonals of Fig. 31. Therefore, the first expected tone in Fig. 32(b) is in the noise floor.

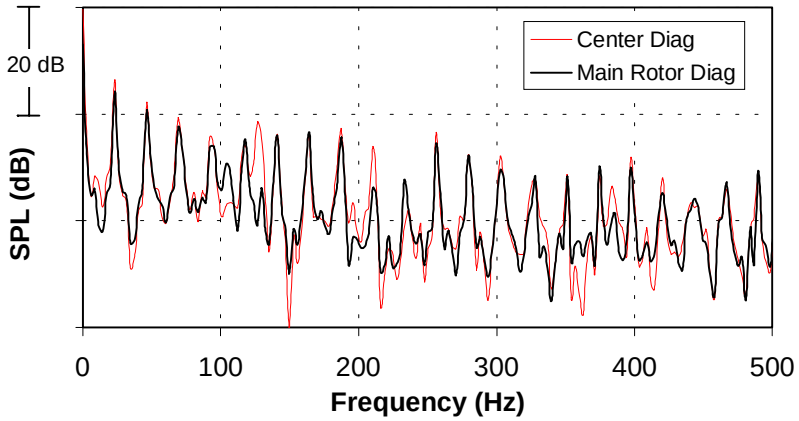

(a) Port Microphone (Retreating side)

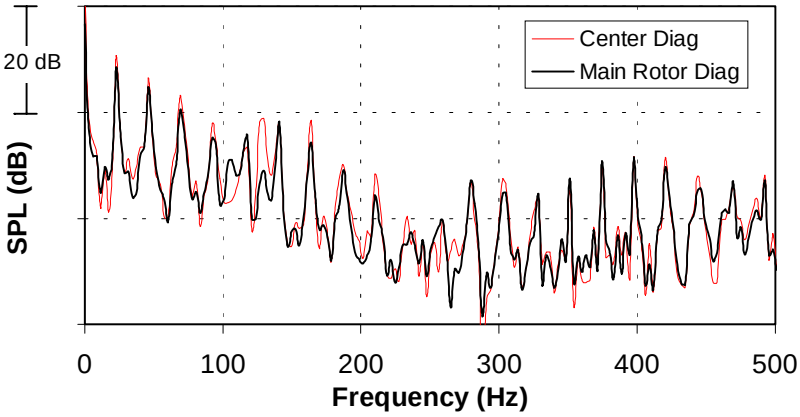

(b) Centerline Microphone

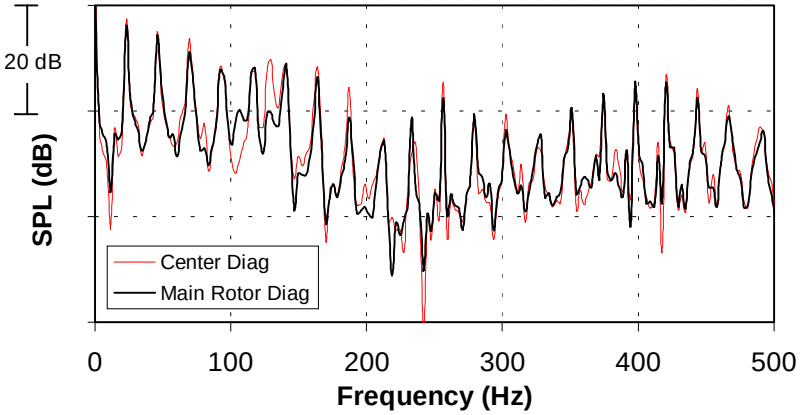

(c) Starboard Microphone (Advancing side)

Figure 31. Center and main rotor diagonals from two-dimensional spectra, Sikorsky S-76C+ 6-deg approach at 74 knots.

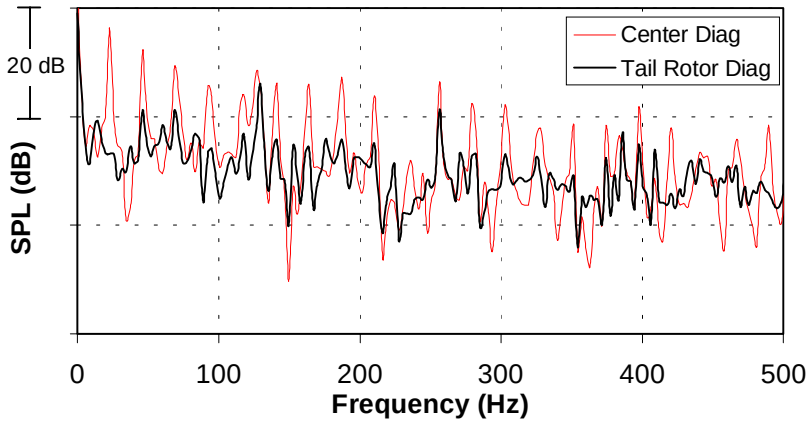

(a) Port Microphone (Retreating side)

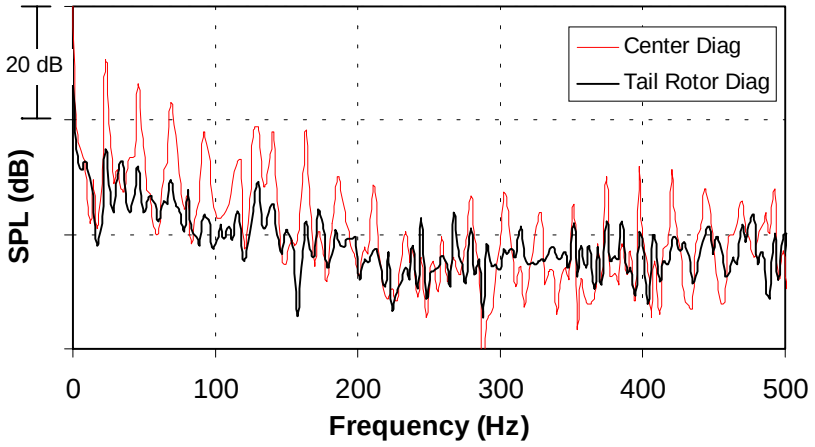

(b) Centerline Microphone

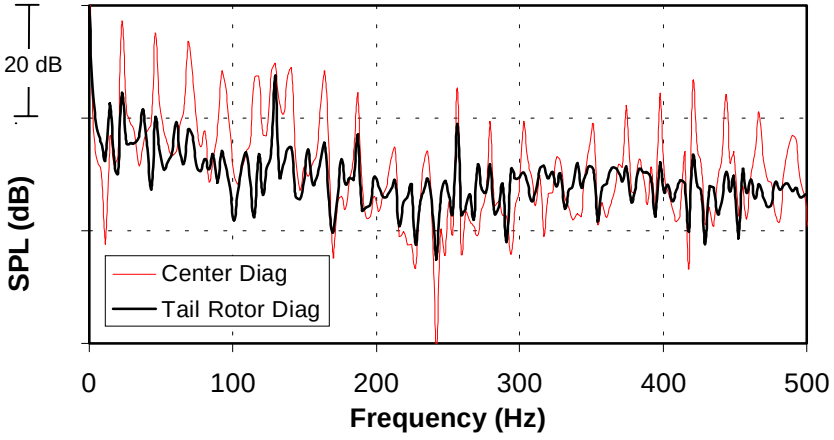

(c) Starboard Microphone (Advancing side)

Figure 32. Center and tail rotor diagonals from two-dimensional spectra, Sikorsky S-76C+ 6-deg approach at 74 knots.

CHAPTER 6

CONCLUSIONS

Two-dimensional Fourier analysis of helicopter flyover noise was found to effectively separate main rotor and tail rotor noise. Since the main rotor and tail rotor frequencies are incommensurate, the resulting signal from a helicopter with a tail rotor is neither periodic nor stationary. A one-dimensional Fourier transform spectrum would not adequately represent these incommensurate frequencies because any data block length chosen would not favor both frequencies.

In this thesis, a method was proposed to separate the main rotor and tail rotor noise spectra. A two-dimensional correlation function was constructed based on a sample record of the noise in the time domain. The two-dimensional Fourier transform of the correlation function was then computed. In these two-dimensional spectra, the main rotor and tail rotor noise spectra are separated from each other on well-defined lines parallel to the center diagonal. This method can separate more than two frequencies as long as they are relatively prime and incommensurate, and was based on ideas suggested in ref. [3].

Data from a helicopter flight test was analyzed using two-dimensional Fourier analysis. The test aircraft were a Boeing MD902 Explorer (no tail rotor) and a Sikorsky S-76C+ (4-bladed tail rotor). The results showed that the main rotor and tail rotor signals can indeed be separated in the two-dimensional Fourier transform spectrum. The separation occurs along the diagonals associated with the frequencies of interest. In most cases shown, the main rotor diagonal was a spectrum dominated by main rotor tones, and the tail rotor diagonal was dominated by tail rotor tones.

There was some unexpected reduction in tail rotor tones in some cases, which could be related to main rotor-tail rotor interaction noise. Information for this type of noise, which is a function of both main rotor and tail rotor frequencies, could also be contained in diagonals corresponding to both frequencies. Looking for evidence of main rotor-tail rotor interaction noise in the two-dimensional spectrum of helicopter noise would be an interesting study for future work.

This method could have applications besides helicopter noise analysis, for example, system identification, monitoring systems, or prediction validation. Although only the amplitudes of the two-dimensional spectra are shown in this thesis, a study of the phase relationships in the two-dimensional spectra could also be useful in these applications. By sweeping through all the diagonals in the two-dimensional spectrum, it may be possible to identify noise sources of interest for system identification. For use in a monitoring system, the diagonal representing the fundamental frequency of a rotating part could be monitored for changes in its periodic motion. To validate noise predictions, one could check for changes in the diagonals of frequencies that are being simulated in the prediction code. In all these examples, two-dimensional Fourier analysis allows frequencies of interest to be separated from the rest of the signal without filters, while retaining access to the rest of the frequency information.

REFERENCES

1) Schmitz, F.H., "Rotor Noise," Chapter 2, *Aeroacoustics of Flight Vehicles: Theory and Practice*, Vol. 1, 1991.

2) George, Albert R., and Chou, S.-T., "A Comparative Study of Tail Rotor Noise Mechanisms," American Helicopter Society 41st Annual Forum, Fort Worth, Texas, May 15–17, 1985.

3) Hardin, J.C., and Miamee, A.G., "Correlation Autoregressive Processes with Application to Helicopter Noise," Journal of Sound and Vibration, 142(2), 1990, pp. 191-202.

4) George, Albert R., Chou, S.-T., "A Comparative Study of Tail Rotor Noise Mechanisms," 41st Annual Forum of the American Helicopter Society, Fort Worth, TX, May 15-17, 1985.

5) George, Albert R., Chou, S.-T., "Helicopter Tail Rotor Analyses," NASA Contractor Report, N86-26163, 1986.

6) Shenoy, R.K., Fitzgerald, J.M., Kohlhepp, F., "Aeroacoustic Investigations of Model Tail Rotors in an Anechoic Wind Tunnel," NASA Contractor Report 181809, 1989.

7) Shenoy, Rajarama K., Moffitt, Robert C., Yoerkie, Charles M., Childress, Otis, Jr., "Development and Validation of 'Quiet Tail Rotor Technology,'" American Helicopter Society International Specialists Meeting on Rotorcraft Acoustics and Fluid Dynamics, Philadelphia, PA, Oct. 15 – 17, 1991.

8) Leverton, John W., Pollard, John S., Wills, Christopher R., "Main Rotor Wake/Tail Rotor Interaction," Vertica, Vol. 1, pp. 213-221, 1977.

9) Hardin, Jay C., *Introduction to Time Series Analysis*, NASA Reference Publication 1145, 2nd printing, Nov. 1990.

10) Bendat, Julius S., Piersol, Allan G., Random Data Analysis and Measurement Procedures, 2nd ed., Wiley, 1986.

11) Smith, Gregory L., "A Two Dimensional Power Spectral Estimate for some Nonstationary Processes," Master's Thesis, Hampton University, Hampton, VA, December 1989.

12) Smith, Gregory L., Miamee, A.G., "A Two-Dimensional Power Spectral Study for some Nonstationary Processes," Proceedings of the Second Workshop on Nonstationary Random Processes and their Applications, San Diego, CA, June 11-12m 1995, World Scientific Publishing Co., Pte. Ltd., 1996.

13 Jacobs, Eric W., O'Connell, James M., Conner, David A., Rutledge, Charles K., Wilson, Mark R., Shigemoto, Fred, Chen, Robert T.N., Fleming, Gregory G., "Acoustic Flight Testing of a Boeing MD Explorer and a Sikorsky S-76B Using a Large Area Microphone Array," American Helicopter Society Technical Specialists Meeting for Rotorcraft Acoustics and Aerodynamics, Williamsburg, VA, October 28 – 30, 1997.

14) JanakiRam, Ram D., O'Connell, James M., Frederickson, Daphne E., Conner, David A., Rutledge, Charles K., "Development and Demonstration of Noise Abatement Approach Flight Operations for a Light Twin-Engine Helicopter – MD Explorer," American Helicopter Society Technical Specialists Meeting for Rotorcraft Acoustics and Aerodynamics, Williamsburg, VA, October 28 – 30, 1997.

15) Jacobs, Eric W., Prillwitz, Ronald D., Chen, Robert T.N., Hindson, William S., Santa Maria, Odilyn L., "The Development and Flight Test Demonstration of Noise Abatement Approach Procedures for the Sikorsky S-76," American Helicopter Society Technical Specialists Meeting for Rotorcraft Acoustics and Aerodynamics, Williamsburg, VA, October 28 – 30, 1997.

APPENDIX A

```
% SGRAM.M
% This macro calculates and plots the spectrogram of a
% flyover.
% Variable name format based on 1996 NRTC test.

% Load data file and define variable name.

flt = num2str(input('Enter flight no: '));
run = num2str(input('Enter run no: '));
mic = num2str(input('Enter mic no: '));

   if str2num(flt)<10
      filen = strcat(['f0',flt,'r',run,'m',mic])
    else
      filen = strcat(['f',flt,'r',run,'m',mic])
   end
      eval(['load ' +filen]);

    if str2num(flt)<10
      varname = strcat(['X0',flt,run,'_',mic,'_time']);
    else
      varname = strcat(['X',flt,run,'_',mic,'_time']);
    end

    eval(['data = ',varname,';']);
    eval(['clear ',varname]);

% Specify input parameters for specgram function
   N = 8192;
   fs = 20000;

% Calculate spectrogram
    b = specgram(data,N,fs,N,N/2);

% Specify parameters for plotting, and plot
   delf = fs/N;
   freq = [0:delf:N/2*delf];
   delt=length(data)/20000/length(b(1,:));
   time=[0:delt:(length(b(1,:))-1)*delt];
   pcolor(time,freq(1:205),20*log10(abs(b(1:205,:))))
   shading interp
   colorbar
```

APPENDIX B

```
% TWODAC.M
% This macro generates the 2-D autocorrelation and
% 2-D spectrum of a signal.
% Input restrictions:
%    N < 2000 for PC/Windows
%    fs/fsd = integer

load data

% Define FFT size, N, and sampling frequency, fs
N = 1776;
fs = 20000;

% Define desired sampling frequency, fsd
fsd = 5000;

% Decimate data
x = decimate(data,fs/fsd);

% Calculate 2-D Autocorrelation, R

for i = [1:N]
   R(i,1:N) = x(i).*x(1:N);
end

S=fft2(R);
```

REPORT DOCUMENTATION PAGE

Form Approved
OMB No. 0704-0188

1. AGENCY USE ONLY (*Leave blank*)	2. REPORT DATE	3. REPORT TYPE AND DATES COVERED
	March 1999	Technical Memorandum

4. TITLE AND SUBTITLE
Two-Dimensional Fourier Transform Applied to Helicopter Flyover Noise

5. FUNDING NUMBERS
WU 581-20-31-01

6. AUTHOR(S)
Odilyn L. Santa Maria

7. PERFORMING ORGANIZATION NAME(S) AND ADDRESS(ES)
NASA Langley Research Center
Hampton, VA 23681-2199

8. PERFORMING ORGANIZATION REPORT NUMBER
L-17827

9. SPONSORING/MONITORING AGENCY NAME(S) AND ADDRESS(ES)
National Aeronautics and Space Administration
Washington, DC 20546-0001

10. SPONSORING/MONITORING AGENCY REPORT NUMBER
NASA/TM-1999-209114

11. SUPPLEMENTARY NOTES
In partial fulfillment of the requirements for the Degree of Master of Science, The Pennsylvania State University, December 1998.

12a. DISTRIBUTION/AVAILABILITY STATEMENT
Unclassified-Unlimited
Subject Category 71 Distribution: Standard
Availability: NASA CASI (301) 621-0390

12b. DISTRIBUTION CODE

13. ABSTRACT *(Maximum 200 words)*
A method to separate main rotor and tail rotor noise from a helicopter in flight is explored. Being the sum of two periodic signals of disproportionate, or incommensurate frequencies, helicopter noise is neither periodic nor stationary, but possibly harmonizable. The single Fourier transform divides signal energy into frequency bins of equal size. Incommensurate frequencies are therefore not adequately represented by any one chosen data block size. A two-dimensional Fourier analysis method is used to show helicopter noise as harmonizable. The two-dimensional spectral analysis method is first applied to simulated signals. This initial analysis gives an idea of the characteristics of the two-dimensional autocorrelations and spectra. Data from a helicopter flight test is analyzed in two dimensions. The test aircraft are a Boeing MD902 Explorer (no tail rotor) and a Sikorsky S-76 (4-bladed tail rotor). The results show that the main rotor and tail rotor signals can indeed be separated in the two-dimensional Fourier transform spectrum. The separation occurs along the diagonals associated with the frequencies of interest. These diagonals are individual spectra containing only information related to one particular frequency.

14. SUBJECT TERMS
fourier transform helicopter flyover noise

15. NUMBER OF PAGES
64

16. PRICE CODE
A04

17. SECURITY CLASSIFICATION OF REPORT	18. SECURITY CLASSIFICATION OF THIS PAGE	19. SECURITY CLASSIFICATION OF ABSTRACT	20. LIMITATION OF ABSTRACT
Unclassified	Unclassified	Unclassified	UL